Palaeoenvironmental reconstructions based on high-resolution oxygen isotope profiles of uppermost Jurassic vertebrate teeth and oyster shells

Hubert Wierzbowski [1],

Błażej Błażejowski [2],

Daniel Tyborowski [3]

[1] Polish Geological Institute – National Research Institute

[2] Institute of Paleobiology, Polish Academy of Sciences

[3] Museum of the Earth in Warsaw, Polish Academy of Sciences

Fot. P. Gieszcz

Location map of the Owadów-Brzezinki quarry in Poland.

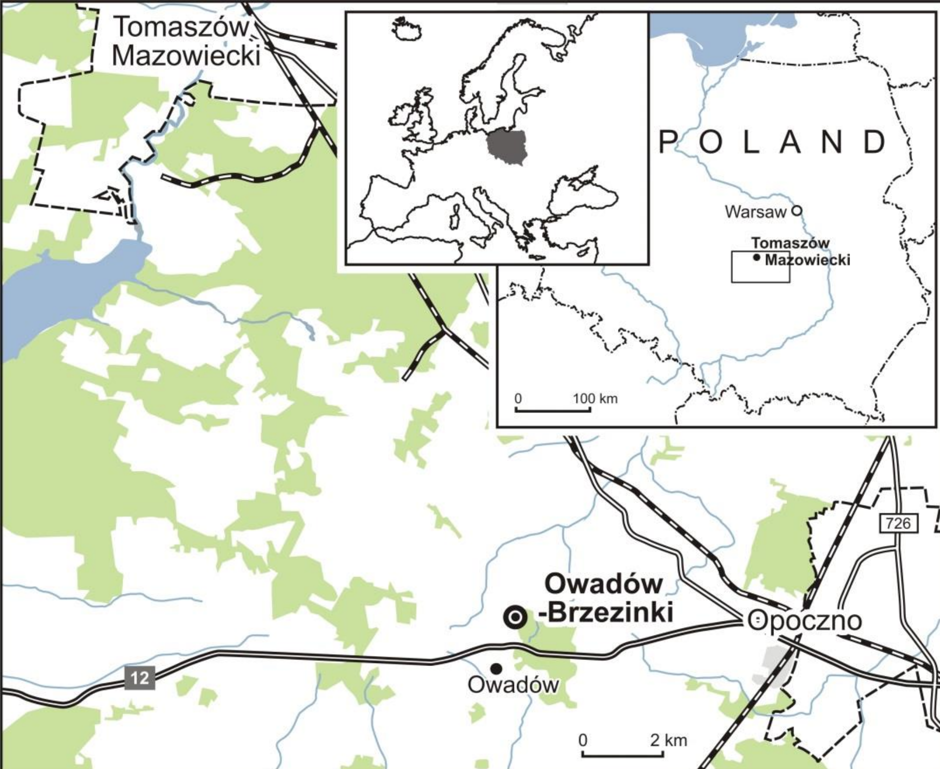

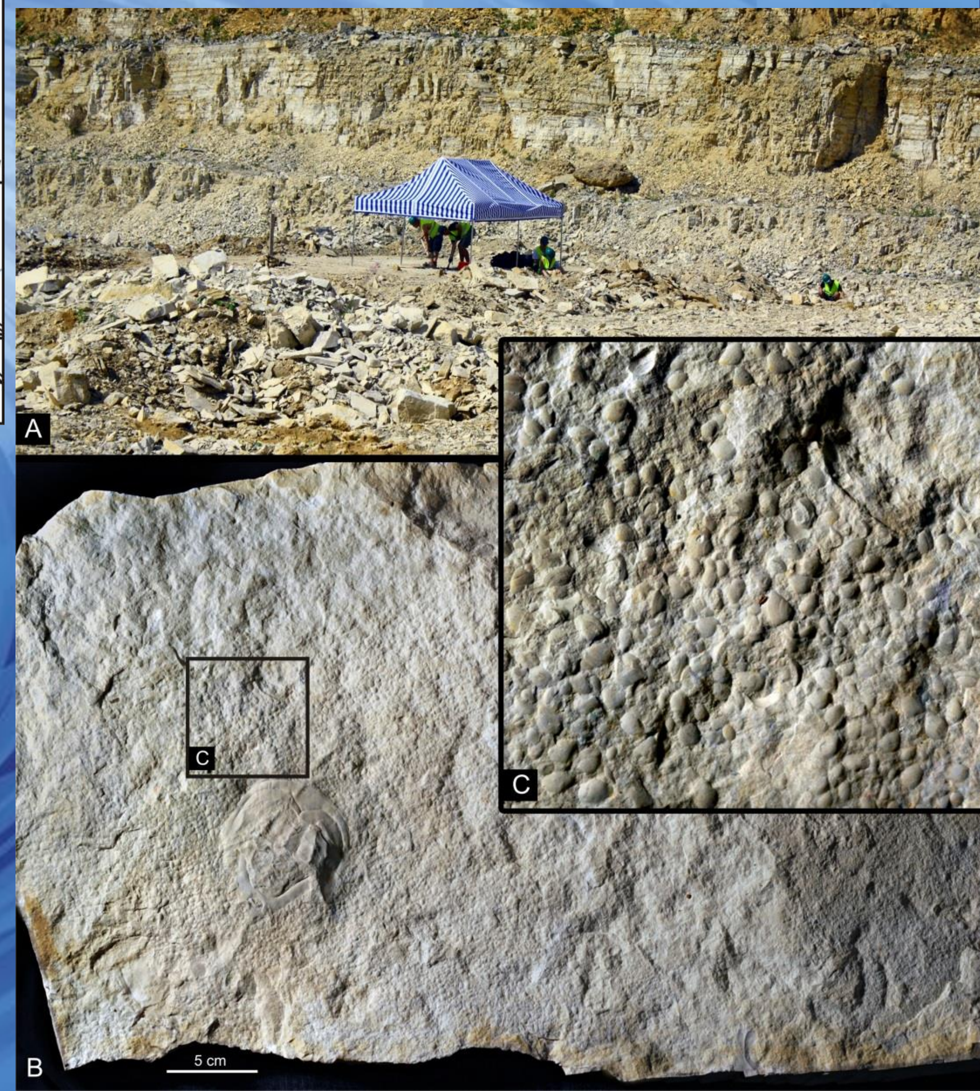

(A) Excavation of the fossiliferous, microbivalve horizon in the middle part the Owadów-Brzezinki quarry, (B) Limestone slab with mass-accumulation of microbivalves and well-preserved limuline horseshoe crab, (C) Abundant representatives of microbivalves.

Lobster-like decapod crustaceans

Comparison between extinct and extant crustaceans sheds new light on several aspects of the evolution of fossil decapods and brings us closer to explanation of the origin of modern decapod crustaceans.

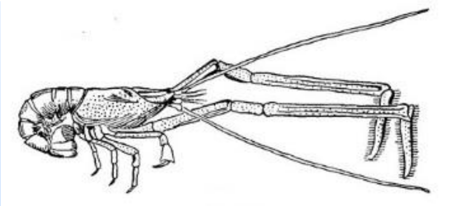

Marine reptiles

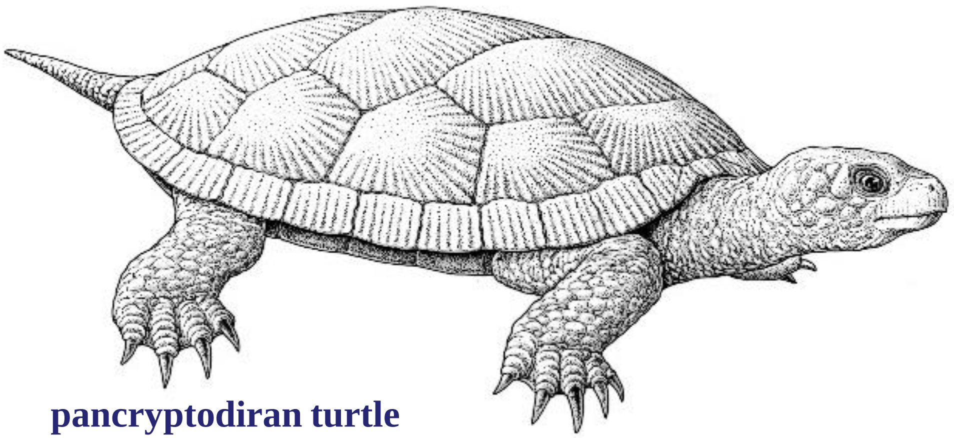

pancryptodiran turtle

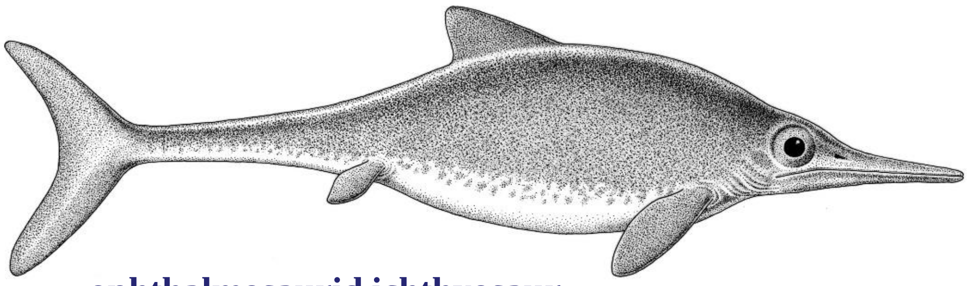

ophthalmosaurid ichthyosaur

Fossil *Limulus darwini* and extant limulines

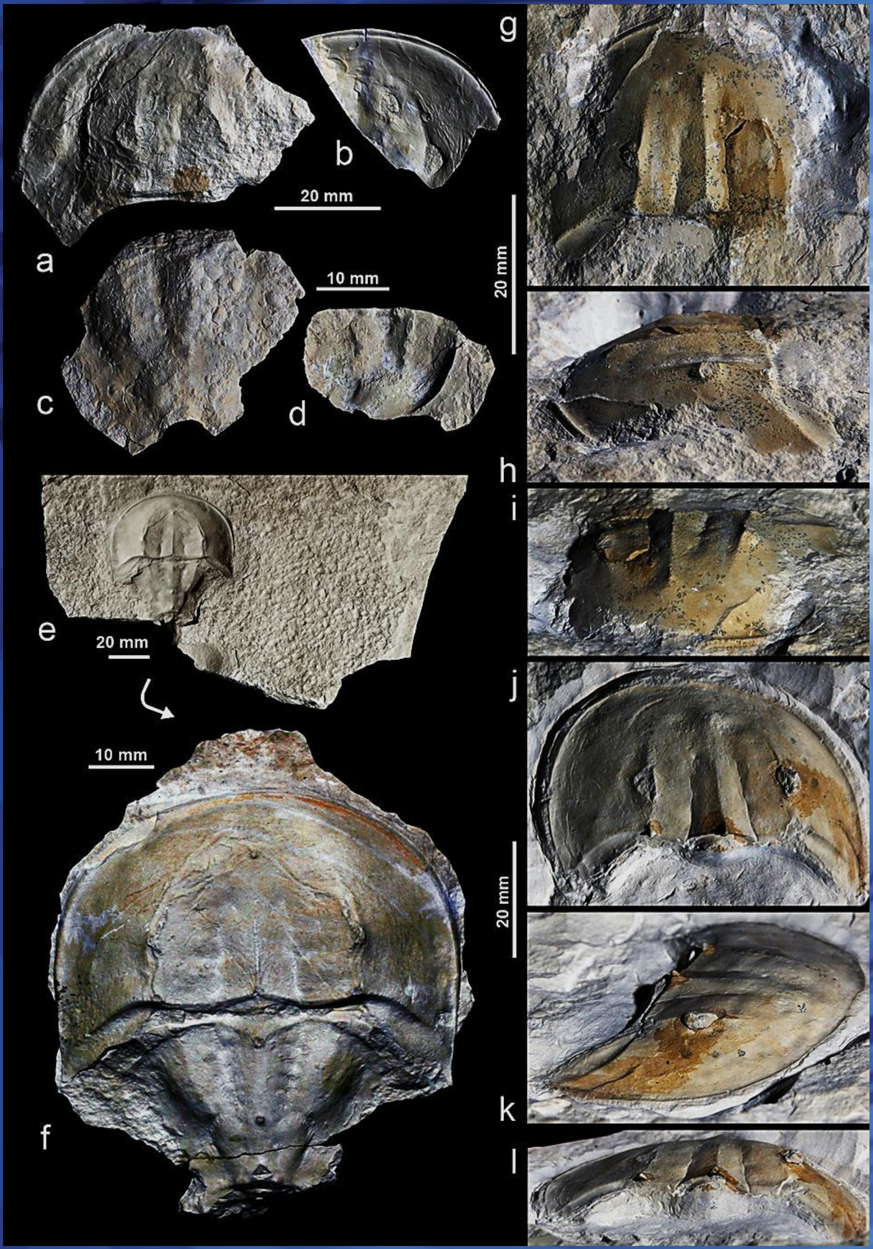

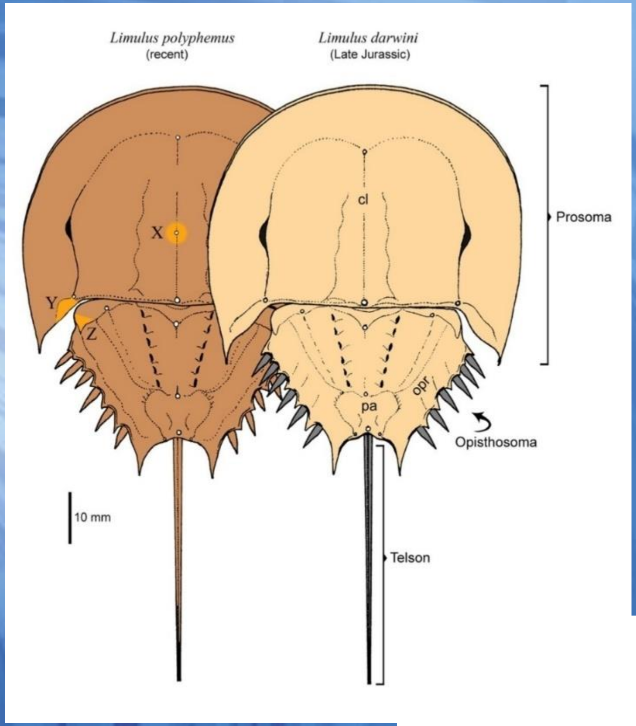

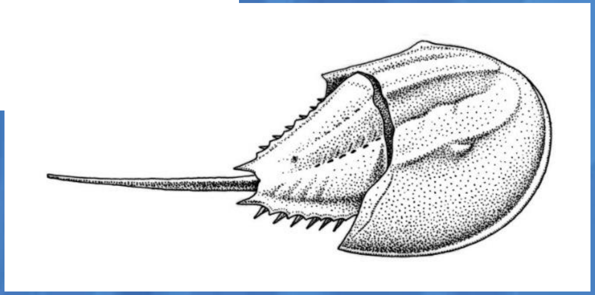

Most substantial morphological difference between fosssil and extant forms.

Owadów-Brzezinki section

Kcynia Formation

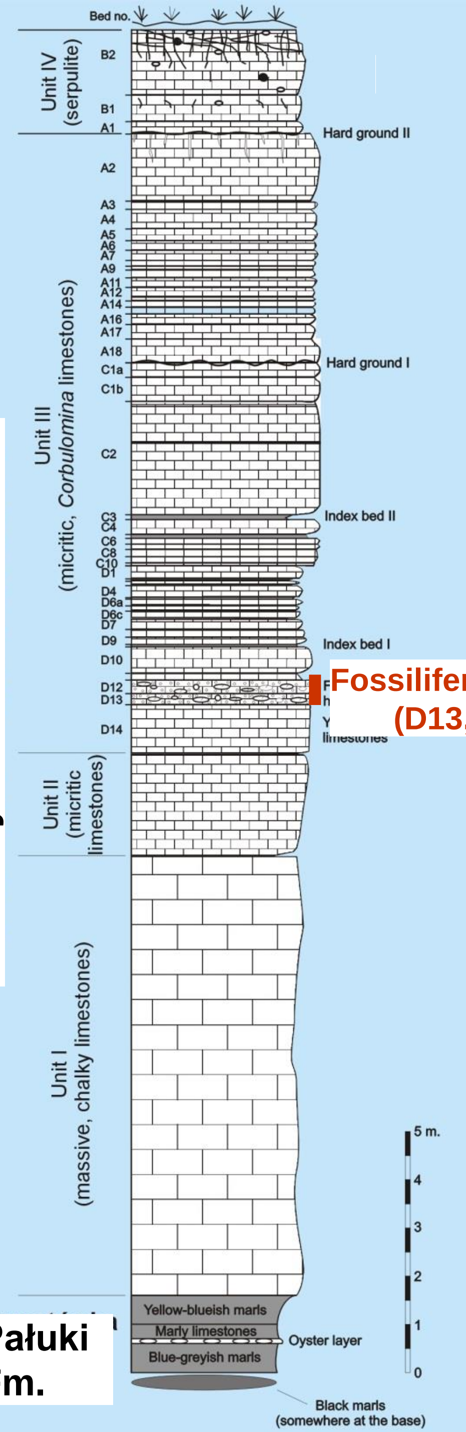

Fossiliferous beds (D13, D12)

Pałuki Fm.

Biostratigraphy of the Owadów-Brzezinki section (after Matyja & Wierzbowski , 2016)

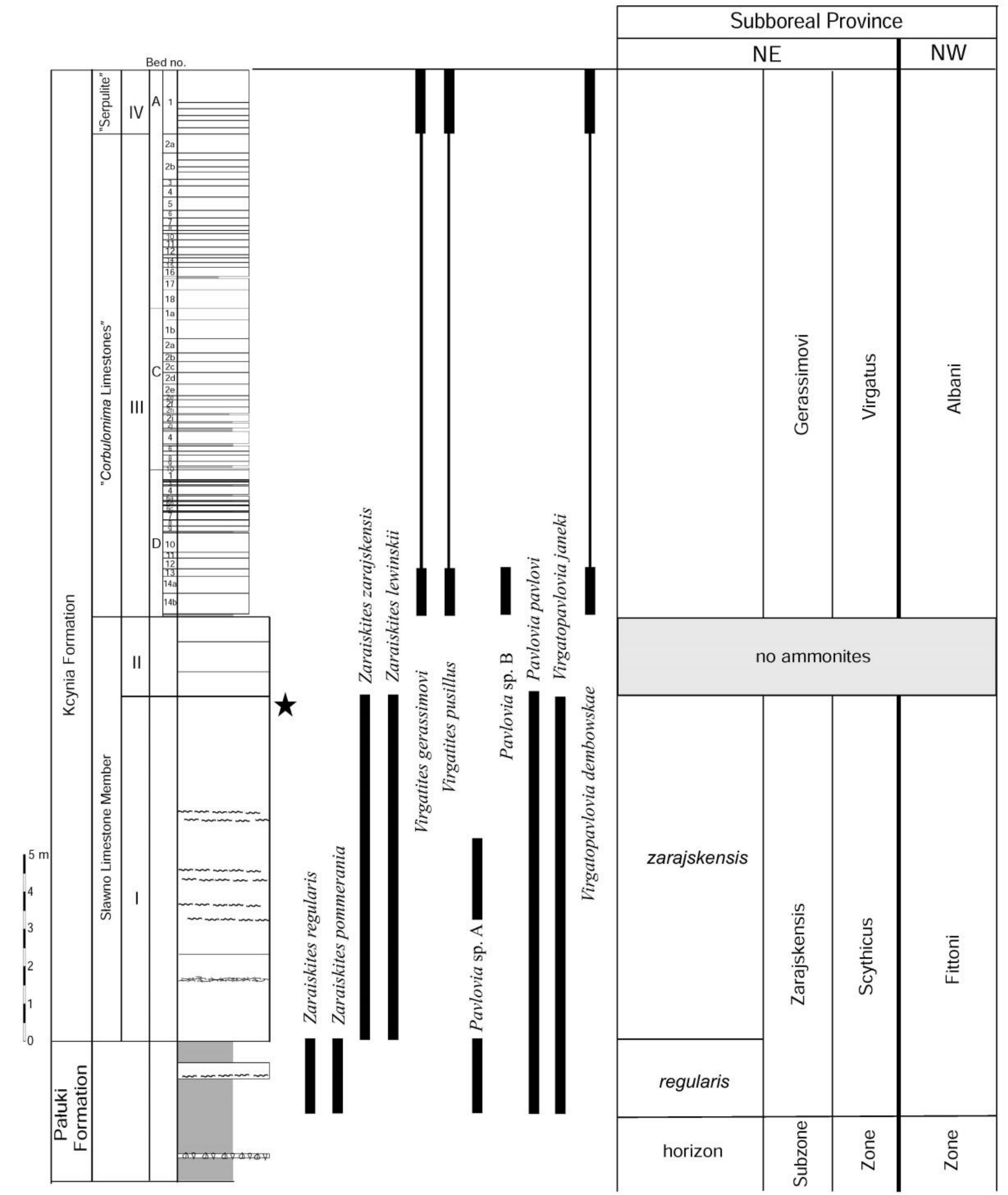

Russian Platform SUB-STAGE	Russian Platform Zone	Russian Platform (Sub)Zone	Position of the base	England, N. France, North Sea STAGE	England, N. France, North Sea Zone	Position of the base	SW Germany, N Italy, Spain SUB-STAGE	SW Germany, N Italy, Spain Zone	SW Germany, N Italy, Spain (Sub)Zone	Position of the base
UPPER VOLGIAN		Singularis	113	PORTLANDIAN	Lamplughi	113	LOWER BERRIASIAN	Jacobi	Grandis	~113
UPPER VOLGIAN	Nodiger	Milkovensis	112	PORTLANDIAN	Preplicomphalus		LOWER BERRIASIAN	Jacobi	Jacobi	112
UPPER VOLGIAN	Nodiger	Nodiger	111	PORTLANDIAN	Preplicomphalus		UPPER TITHONIAN	Jacobi	Jacobi	~111.13
UPPER VOLGIAN		Catenulatum	110	PORTLANDIAN	Preplicomphalus	~107.73	UPPER TITHONIAN		Durangites	~109.11
UPPER VOLGIAN	Fulgens	Subfulgens	109	PORTLANDIAN	Preplicomphalus		UPPER TITHONIAN		Durangites	
UPPER VOLGIAN	Fulgens	Fulgens	108	PORTLANDIAN	Preplicomphalus		UPPER TITHONIAN		Microcanthum	
MIDDLE VOLGIAN	Nikitini	Nikitini	107	PORTLANDIAN	Primitivus	~107.25	UPPER TITHONIAN		Microcanthum	
MIDDLE VOLGIAN	Nikitini	Lahuseni	106	PORTLANDIAN	? Oppressus / Anguiformis	~106.42 / 105.82	UPPER TITHONIAN		Microcanthum	
MIDDLE VOLGIAN	Nikitini	Bipliciformis	105	PORTLANDIAN	Kerberus	105.30	UPPER TITHONIAN		Microcanthum	101.86
MIDDLE VOLGIAN	Virgatus	Rosanovi	104	PORTLANDIAN	Okusensis	104.42	UPPER TITHONIAN		Microcanthum	
MIDDLE VOLGIAN	Virgatus	Virgatus	103	PORTLANDIAN	Glaucolithus	102.81	UPPER TITHONIAN		Microcanthum	
MIDDLE VOLGIAN	Virgatus	Gerassimovi	102	PORTLANDIAN	Albani	102	UPPER TITHONIAN		Microcanthum	
MIDDLE VOLGIAN	Panderi	Zarajskensis	101	BOLONIAN	Fittoni	101.19	LOWER TITHONIAN		Palmatus (= Ponti)	100.02
MIDDLE VOLGIAN	Panderi	Scythicus	100	BOLONIAN	Rotunda / Pallasioides	100.67 / 100.06	LOWER TITHONIAN		Palmatus (= Ponti)	
LOWER VOLGIAN	Pseudo-scythica	Puschi	99	BOLONIAN	Pectinatus	98.39	LOWER TITHONIAN		Ciliata (= Fallauxi + Semiforme)	98.32
LOWER VOLGIAN	Pseudo-scythica	Pseudoscythica	98	BOLONIAN	Hudlestoni	97.88	LOWER TITHONIAN		Ciliata (= Fallauxi + Semiforme)	
LOWER VOLGIAN		Sokolovi	97	BOLONIAN	Wheatleyensis	97.29	LOWER TITHONIAN	Dar-wini	Vimineus / Mucronatum	97.62 / 97.14
LOWER VOLGIAN		Klimovi	96	BOLONIAN	Scitulus / Elegans	96.61 / 96	LOWER TITHONIAN	Hybo-notum	Moernsheimensis / Rupelianum / Riedense	96.56 / 96.33 / 96

J-K boundary (calpionellid)

Owadów-Brzezinki section

Corelation between uppermost Jurassic zonal schemes (after Wierzbowski et al., 2017)

Presence of benthic foraminifera, ostracods, echinoderms, prasinophycean alga and pseudomorphs after gypsum in the Owadów-Brzezinki section (after Wierzbowski et al. 2016)

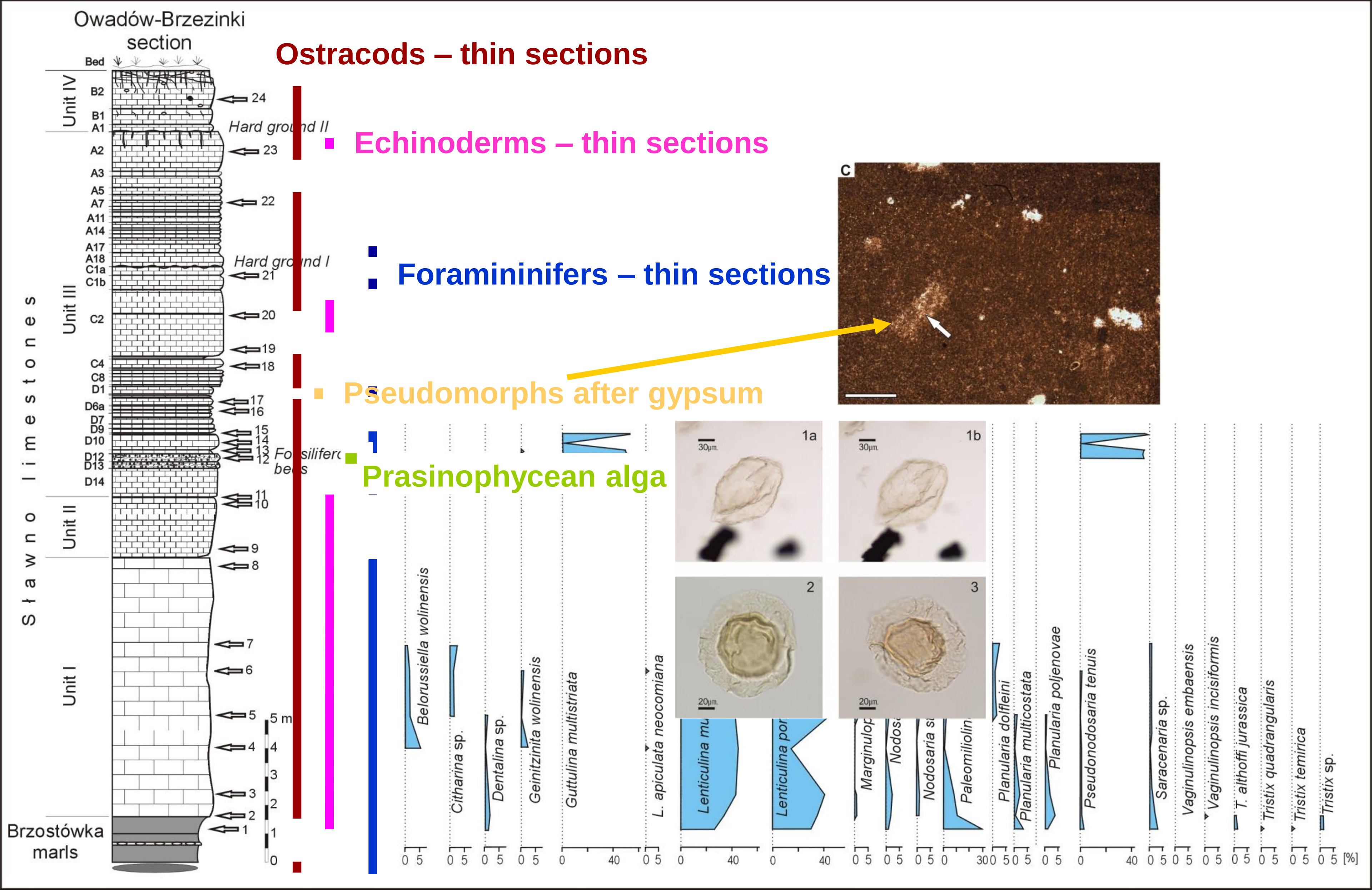

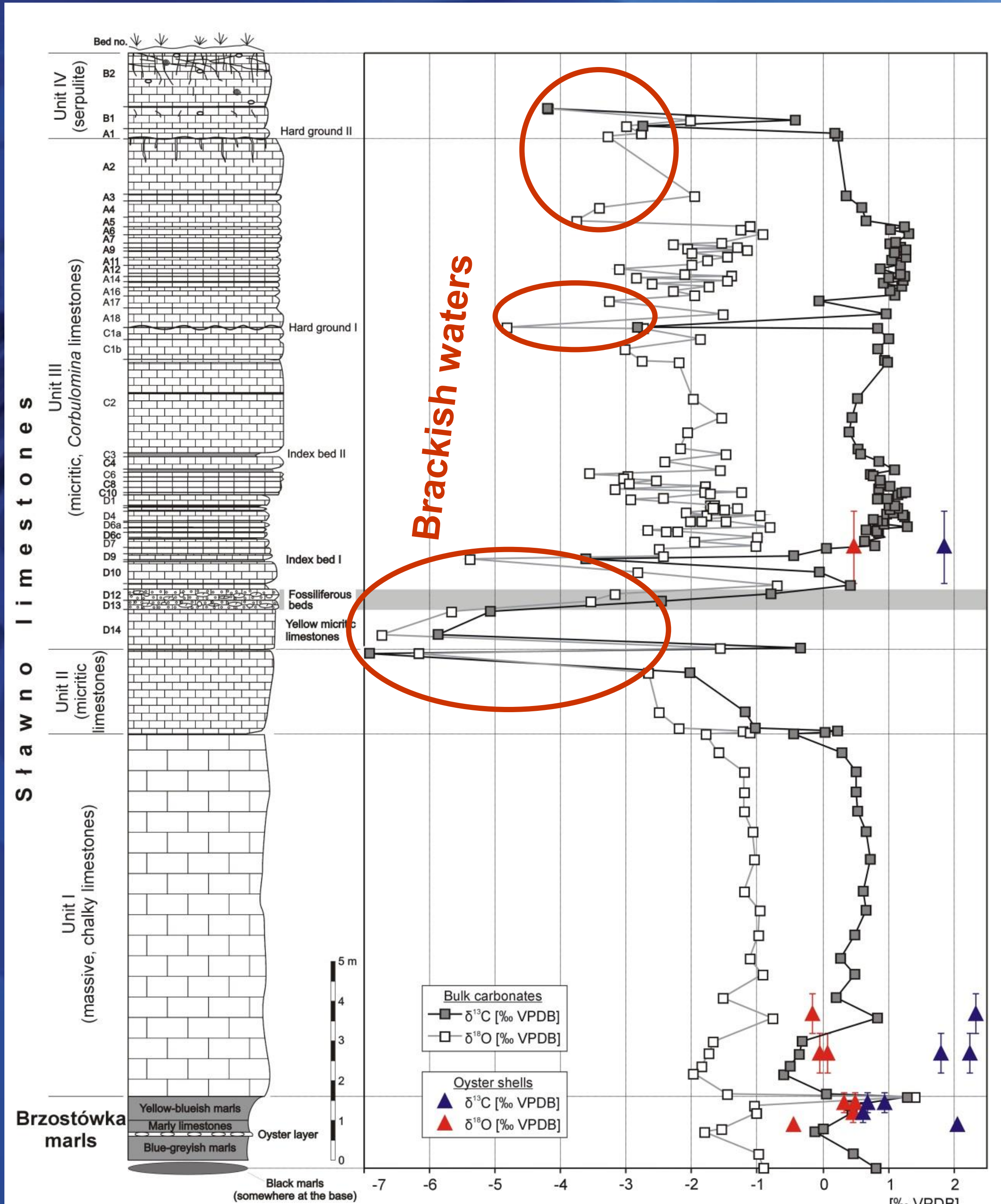

Lithology, $\delta^{13}C$ and $\delta^{18}O$ values of bulk carbonates from the Owadów-Brzezinki section.

$\delta^{18}O$ versus $\delta^{13}C$ values of bulk carbonates from the Owadów-Brzezinki section. Correlation (r^2=0.52) between $\delta^{18}O$ and $\delta^{13}C$ values is statistically significant.

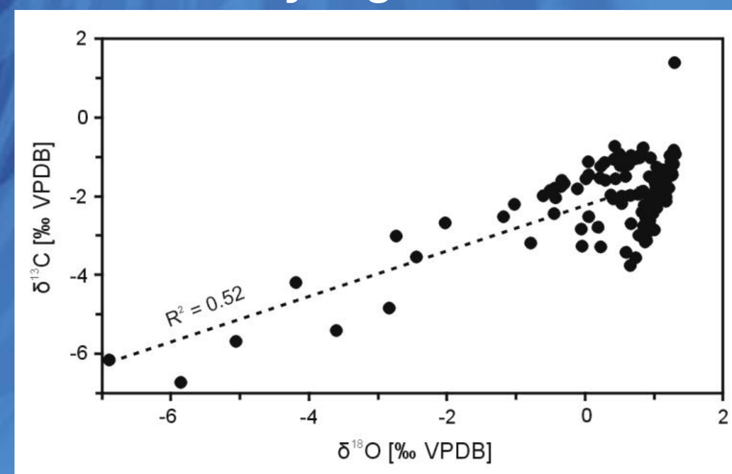

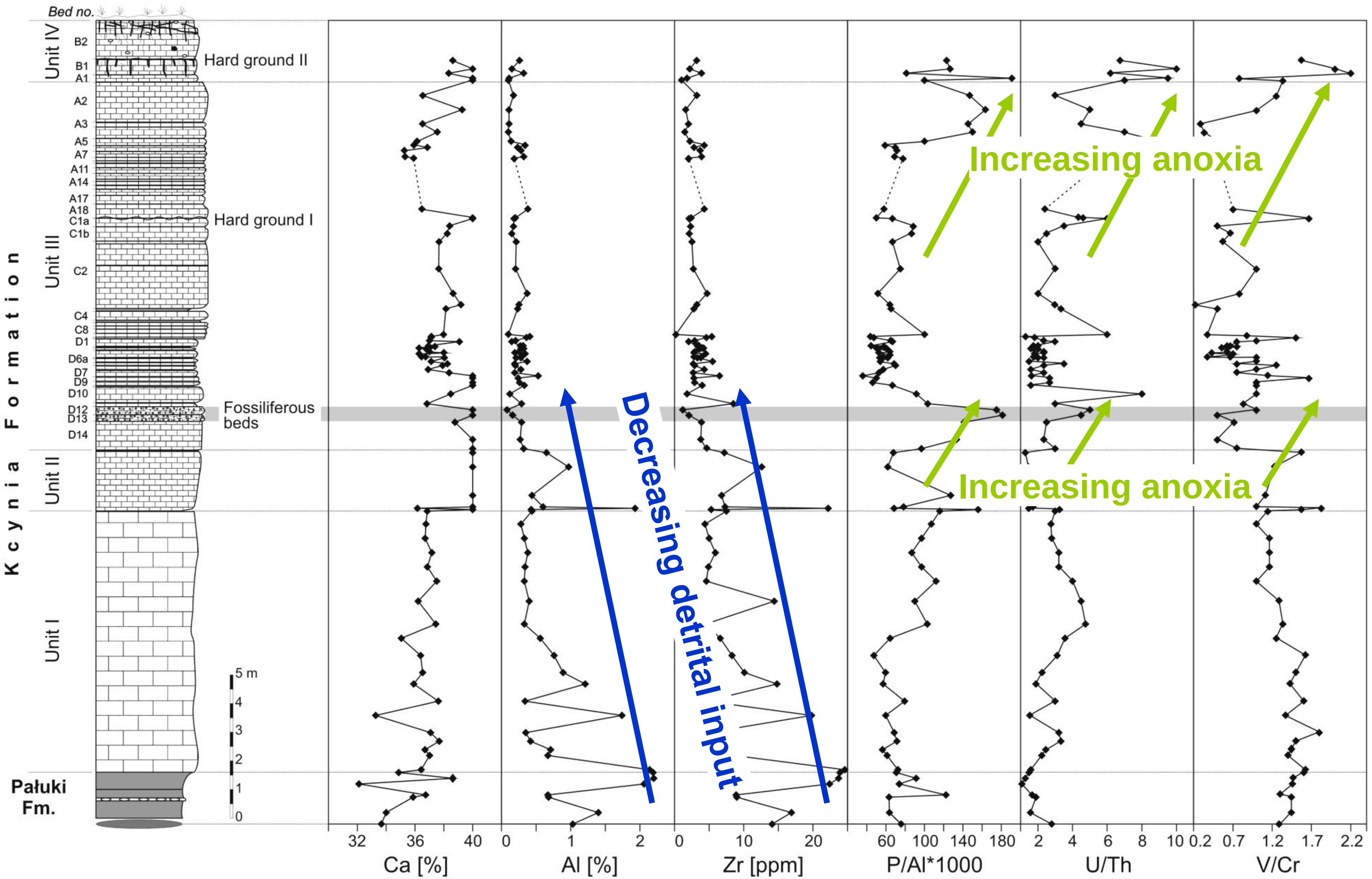

Lithology, Ca, Al, Zr concentrations, and P/Al, U/Th, V/Cr ratios of bulk carbonates from the Owadów-Brzezinki section.

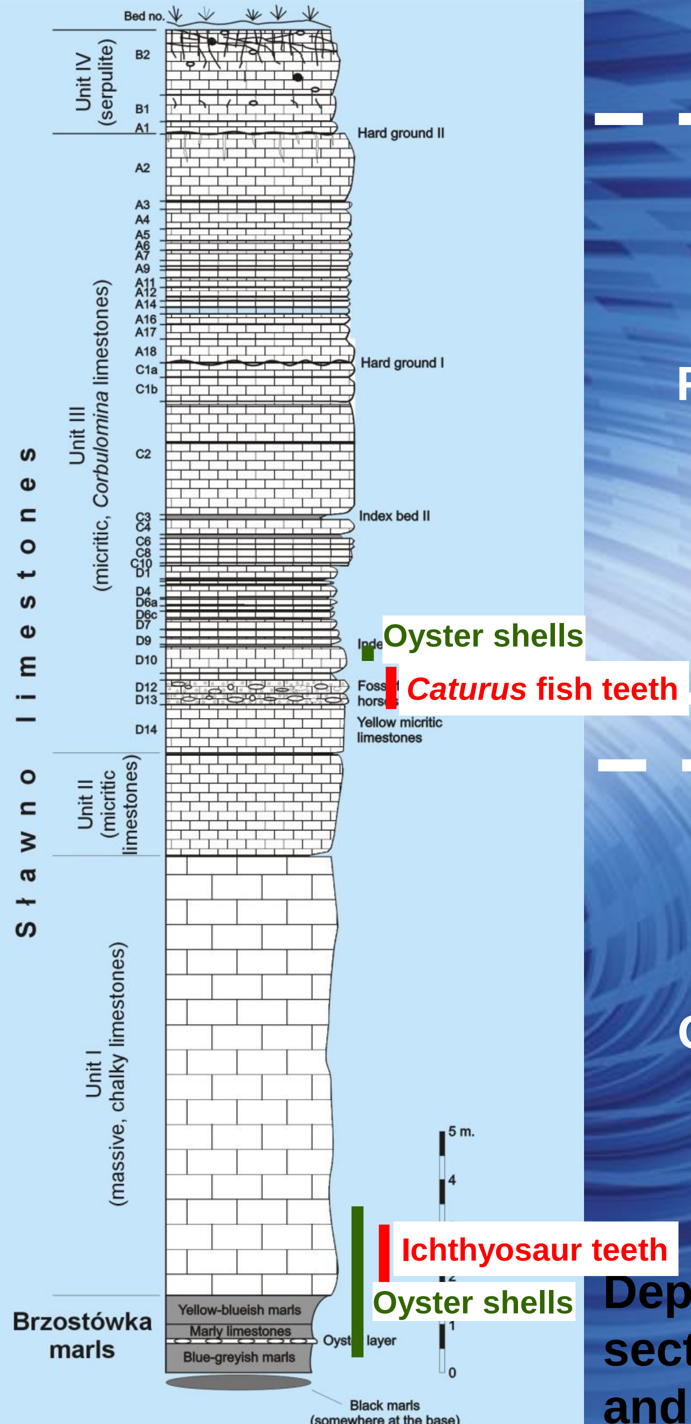

Coastal settings, normal marine salinity

Restricted lagoon, variations in salinities and oxygenation level of bottom waters

Coastal settings, brackish waters

Offshore to nearshore settings, normal marine salinity

Depositional environments of the Owadów-Brzezinki section (after Kin et al. 2013; Wierzbowski et al. 2016) and samples collected for isotope studies

Chemical and isotope data of oyster (*Deltoideum delta*) shells from the Owadów-Brzezinki section (after Wierzbowski et al. 2016)

Sample	Unit/ bed	Fe (ppm)	Mn (ppm)	Sr (ppm)	$\delta^{13}C$ (‰ VPDB)	$\delta^{18}O$ (‰ VPDB)
SHW119	Unit II/ beds D4-D10	<100	14	556	1.85	0.47
SHW132	Unit I/ ca. 2.0 m above the base	<100	15	511	2.33	-0.16
SHW108	Unit I/ ca. 1.0 m above the base	<100	16	469	1.80	-0.05
SHW124	Unit I/ ca. 1.0 m above the base	<100	12	464	2.24	0.07
SHW125	Pałuki Formation/ ca. 0.25 m below the top	215	13	656	0.94	0.49
SHW126	Pałuki Formation / ca. 0.25 m below the top	<100	29	609	0.68	0.32
SHW118	Pałuki Formation / ca. 0.5 m below the top	137	28	612	0.61	0.46
SHW110	Pałuki Formation/ oyster layer	112	26	499	2.05	-0.45

Well-preserved oyster shells are characterized by dull to medium cathodoluminescence, low Mn, Fe and high Sr concentrations (Mn < 100 ppm, Fe < 250 ppm, and Sr > 490 ppm; Wierzbowski et al. 2016)

$\delta^{18}O$ values of well-preserved bulk oyster shells vary between -0.5 and 0.5‰ (mean 0.1‰) VPDB (Wierzbowski et al. 2016)

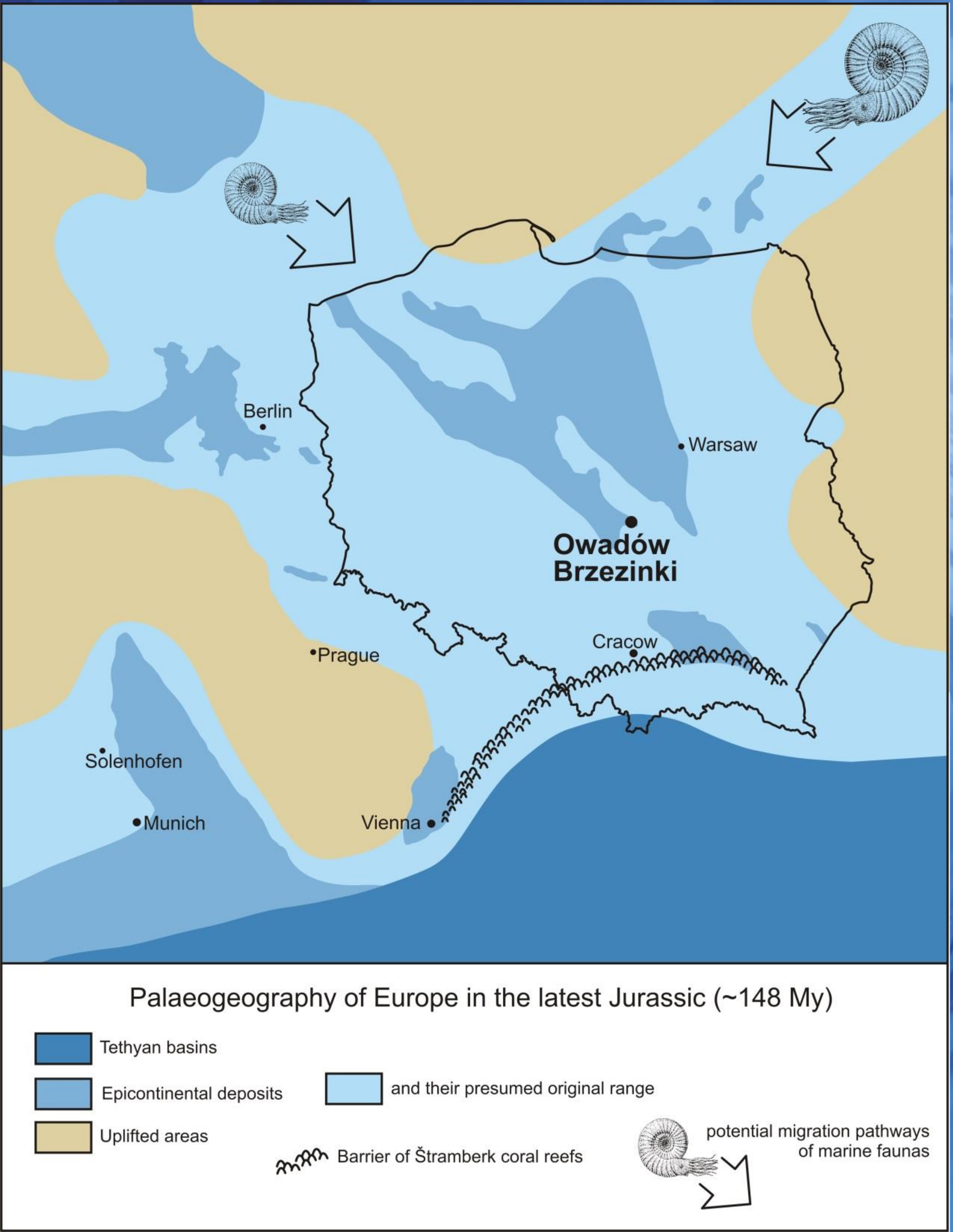

Palaeogeography of the mid-Polish basin allowed fauna migrations e.g. some ammonite genera as *Virgatopavlovia* are common with southern England, whereas others as *Zaraiskites* and *Virgatites* are forms typical of the Russian Platform

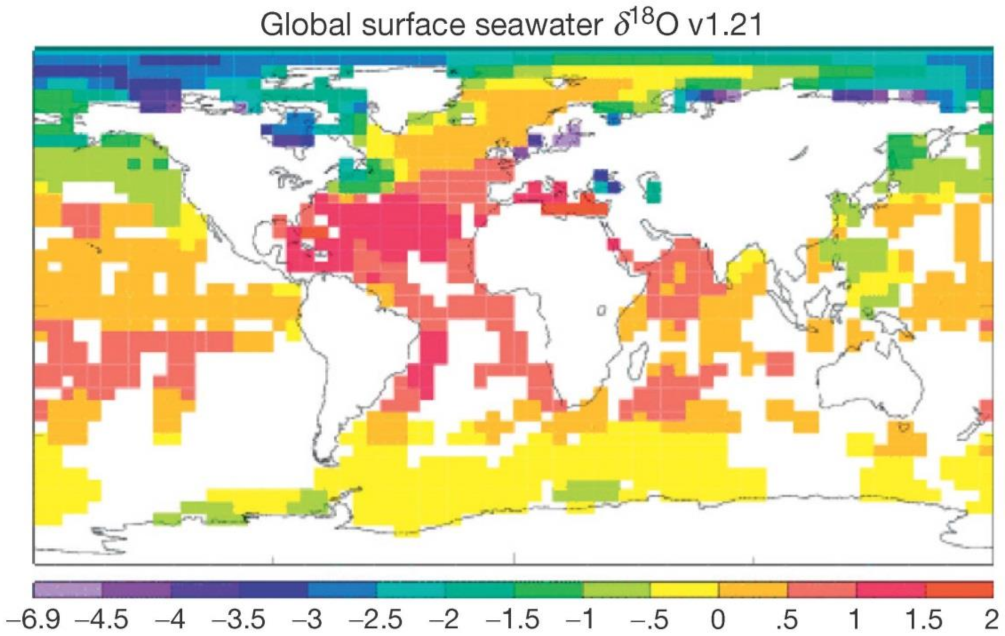

Mean annual $\delta^{18}O$ values of modern surface seawater (after Rohling, 2013)

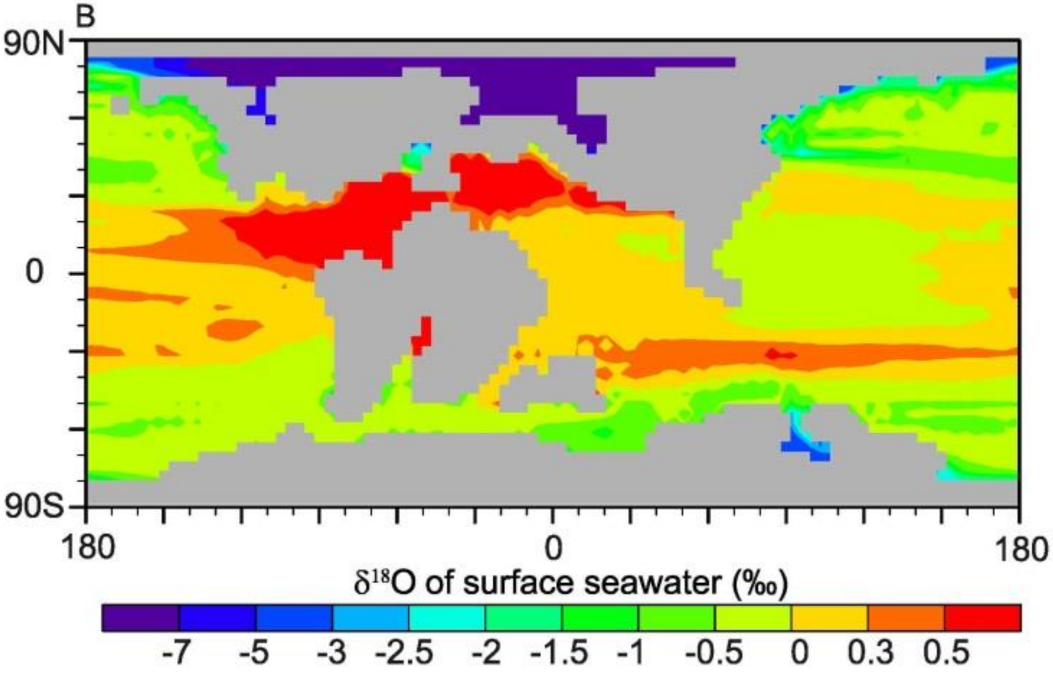

Mean annual $\delta^{18}O$ values of Cretaceous surface seawater (a K-Bathy model of Zhou et al. 2008)

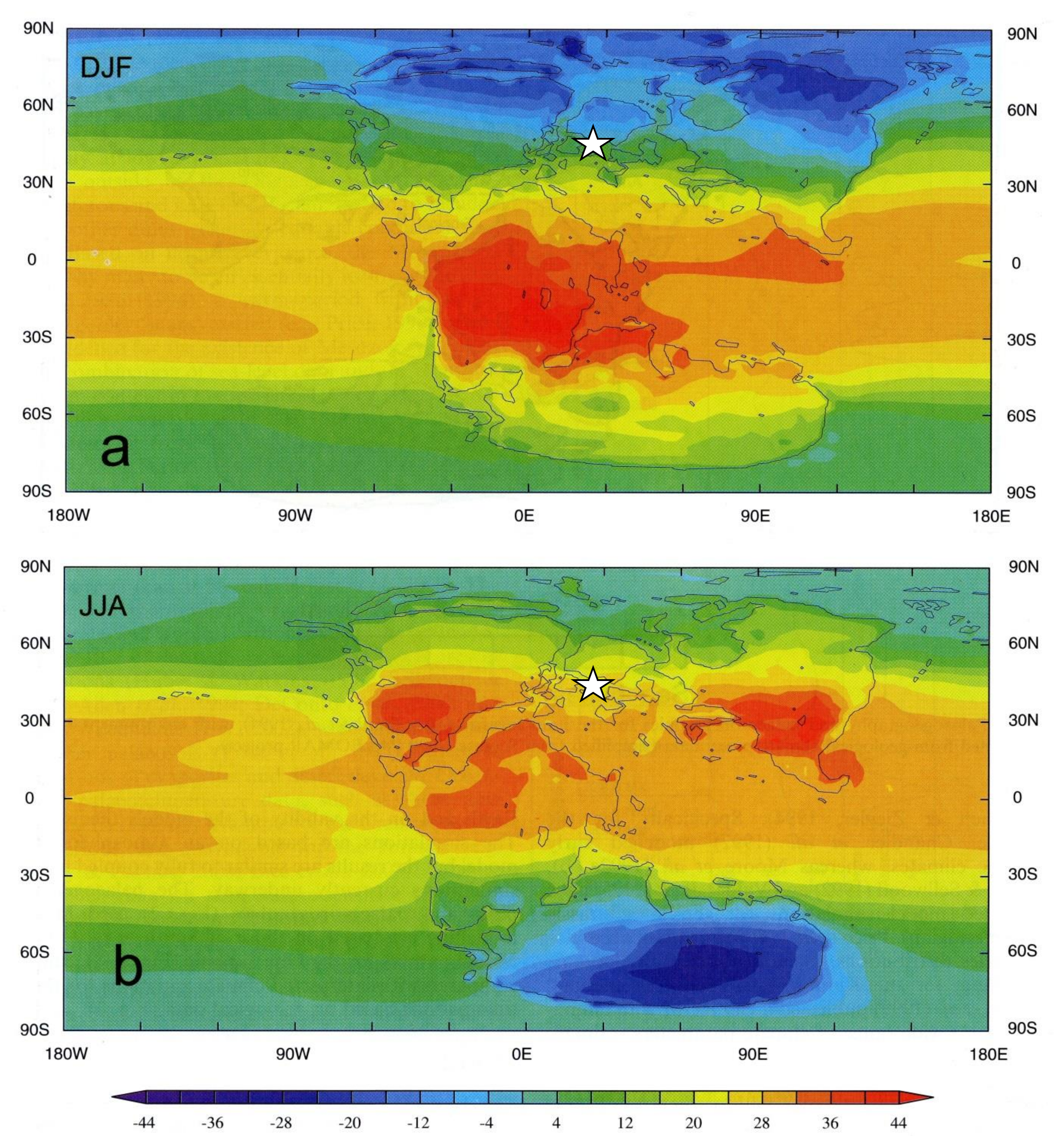

Winter – N Nemisphere

Summer – N Hemisphere

Mean temperatures at sea surface in the Late Jurassic (a palaeoclimatic model of Sellwood & Valdes, 2008; white star – Owadów-Brzezinki site)

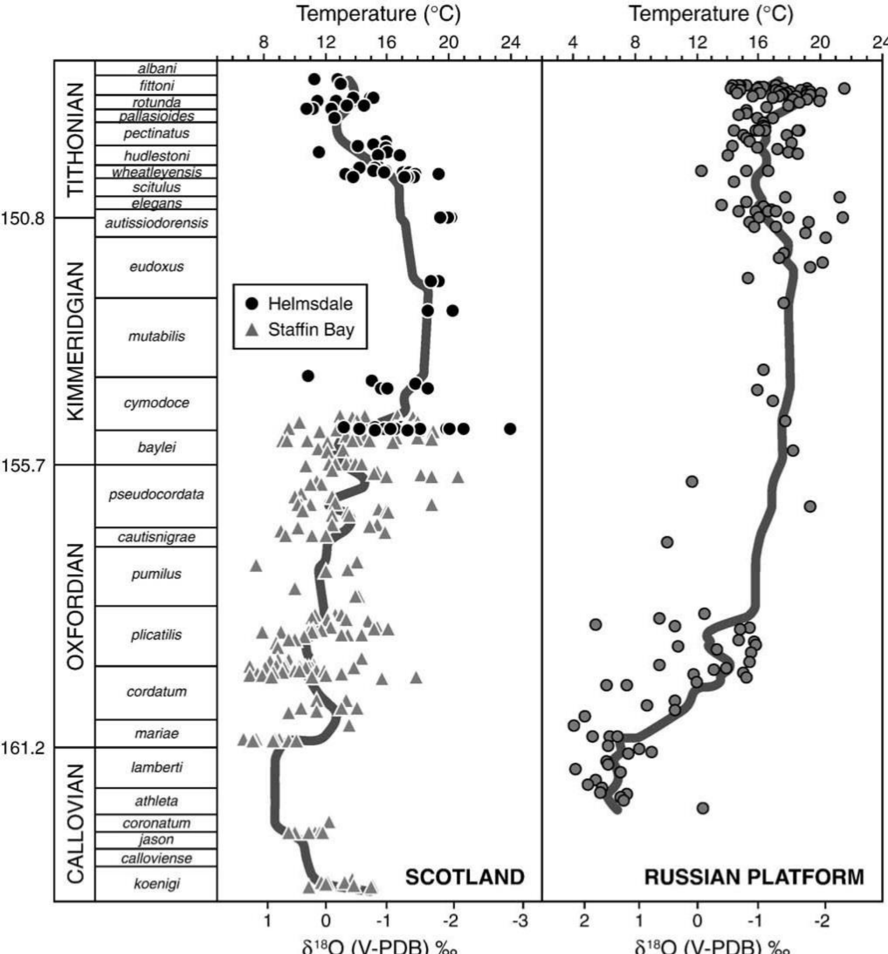

Summary of Callovian–Tithonian belemnite $\delta^{18}O$ values and palaeo-temperatures from Scotland and the Russian Platform (after Nunn & Price, 2010).

Salinity–$\delta^{18}O_{seawater}$ model for the Owadów-Brzezinki site (after Wierzbowski et al. 2016). The measured range of $\delta^{18}O_{oyster}$ (from -0.45 to 0.49‰) and assumed temperatures of ambient waters (11 to 17ºC) translate into palaeosalinities of 31.5 to 39.1 ppt (using a model of Railsback et al., 1989).

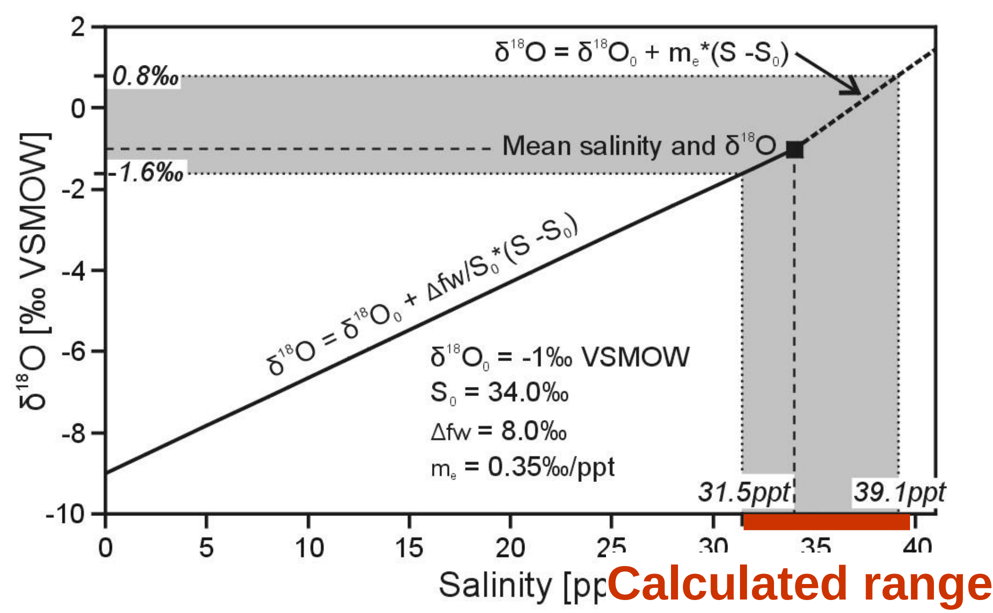

Oyster shells (*Deltoideum delta*)

MicroMill micro-sampling device

Ichthyosaur teeth (*Cryopterygius kielanae*)

Fish teeth (*Caturus* sp.)

SHRIMP IIe/MC ion microprobe

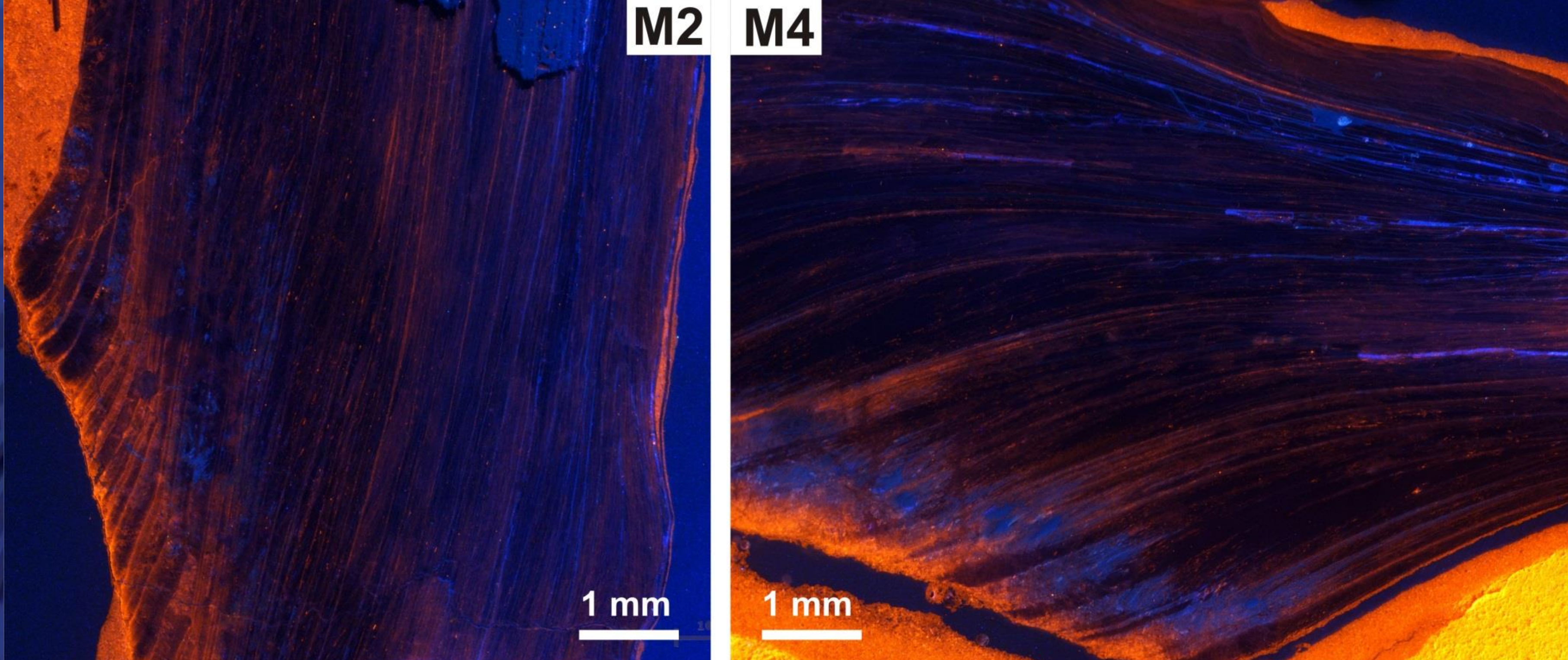

Cold cathodoluminescence images of ligamental areas of *D. delta* oysters which were microsampled for oxygen and carbon isotopes using a MicroMill.

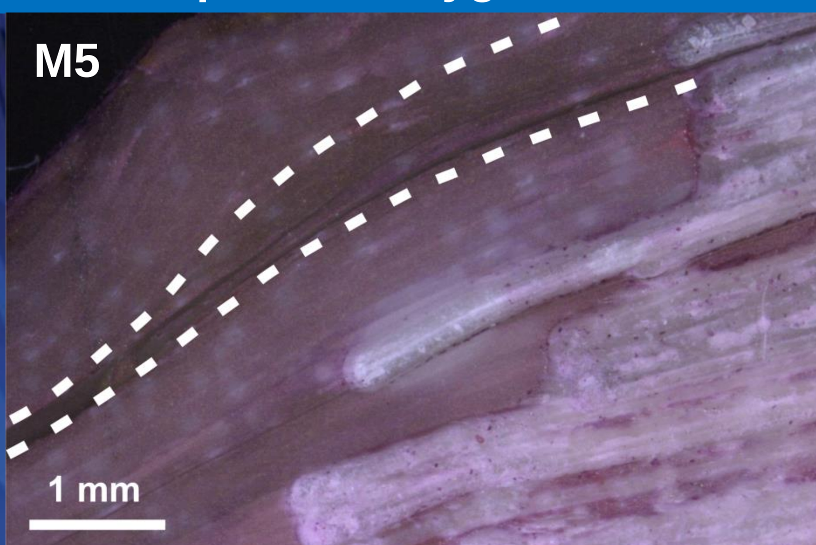

Oyster stained with Evamy's solution. Darker band is related to increased Fe content

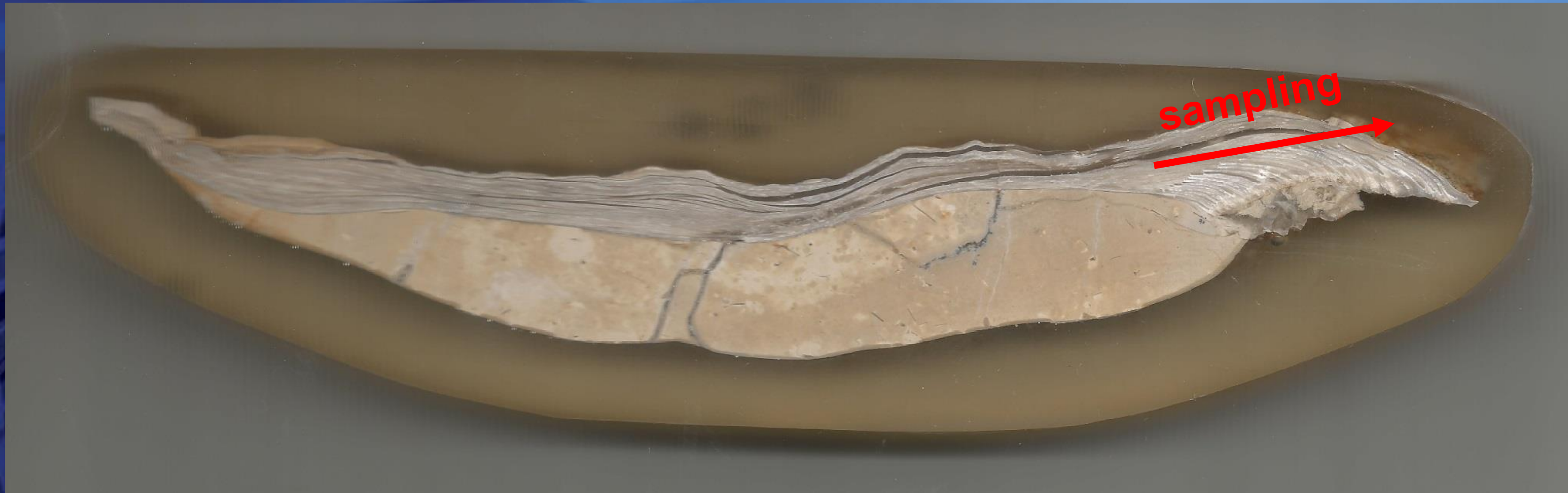

Oyster shell (specimen M2a; *D. delta*) sampled in a ligamental area (at ca. 0.5 mm intervals) for O and C isotopes, using a MicroMill device

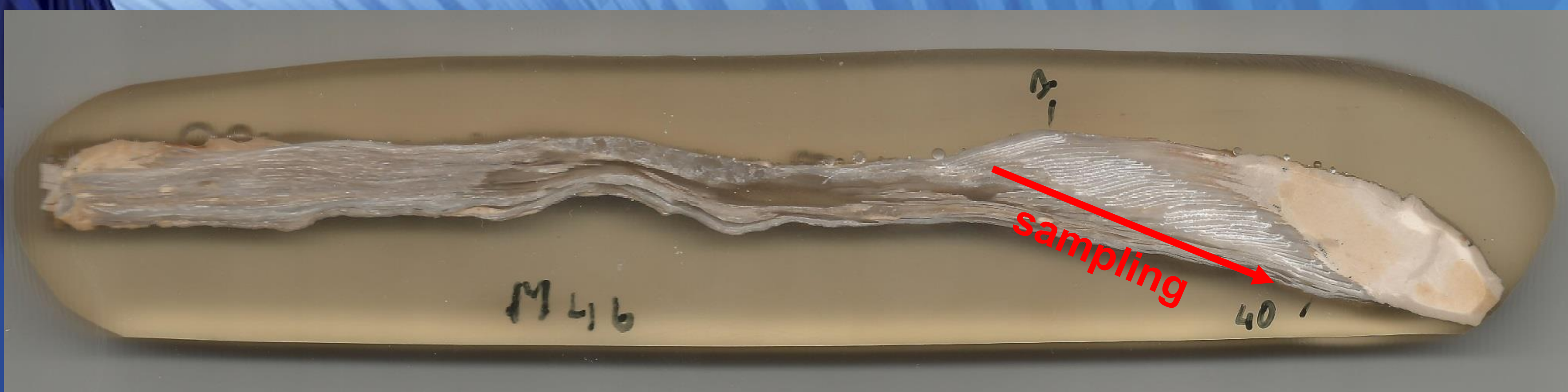

Oyster shell (specimen M4b; *D. delta*) sampled in a ligamental area (at ca. 0.5 mm intervals) for O and C isotopes, using a MicroMill device

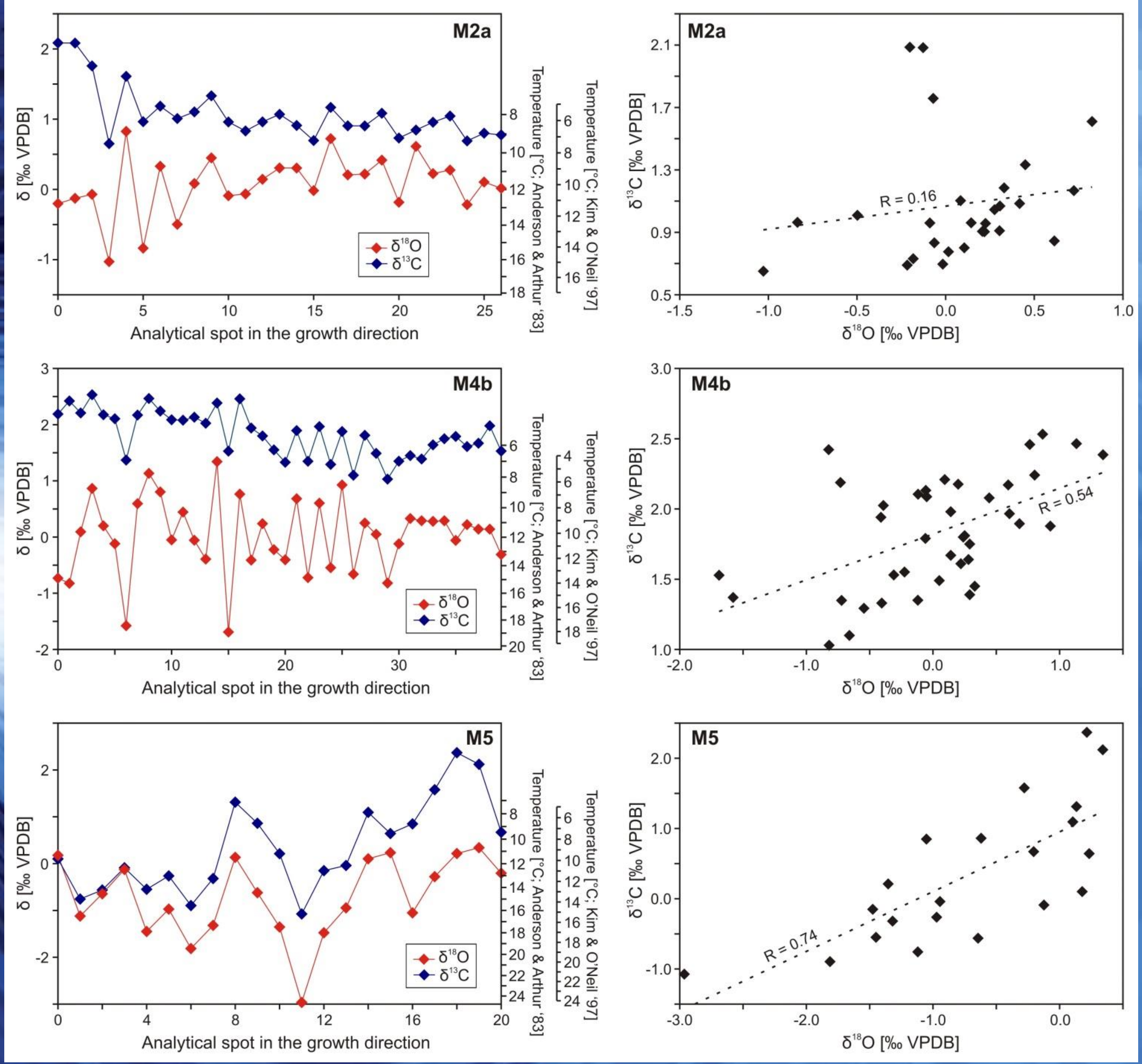

Ontogenetic $\delta^{18}O$ and $\delta^{13}C$ profiles from ligamental areas of oyster shells and correlations between isotope values. Absolute temperatures are calculated from palaeotemperature equations assuming $\delta^{18}O_{water}$ = -1‰ VSMOW.

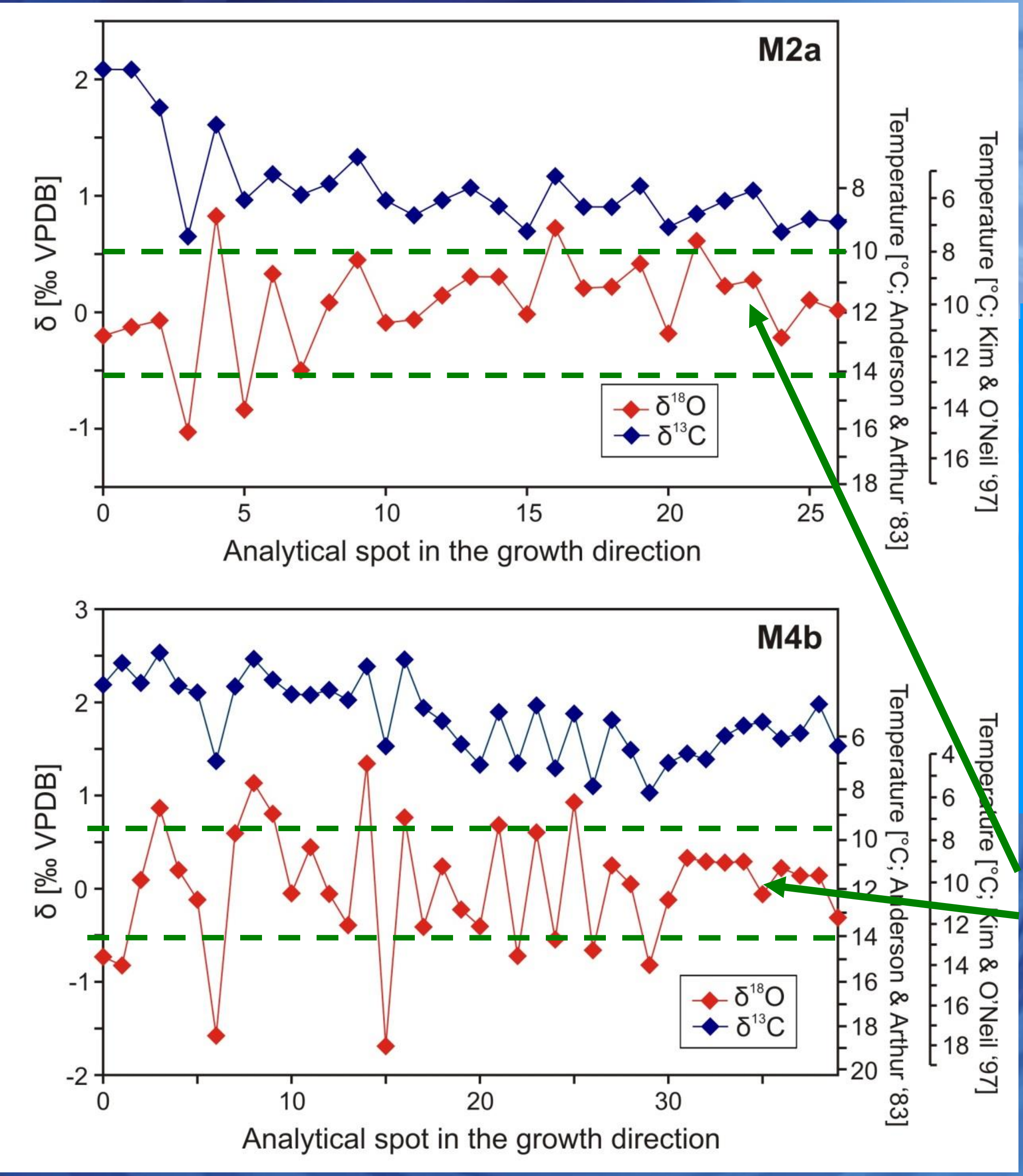

$\delta^{18}O$ and $\delta^{13}C$ values of transverse section throughout the ligamental area of oyster shells (*D. delta*). Absolute temperatures are calculated using Anderson & Arthur (1983) and Kim & O'Neil (1997) equations and an asumption of $\delta^{18}O_{seawater}$ = -1‰ VSMOW.

Range of $\delta^{18}O$ of bulk oyster shells (data published in Wierzbowski et al. 2016)

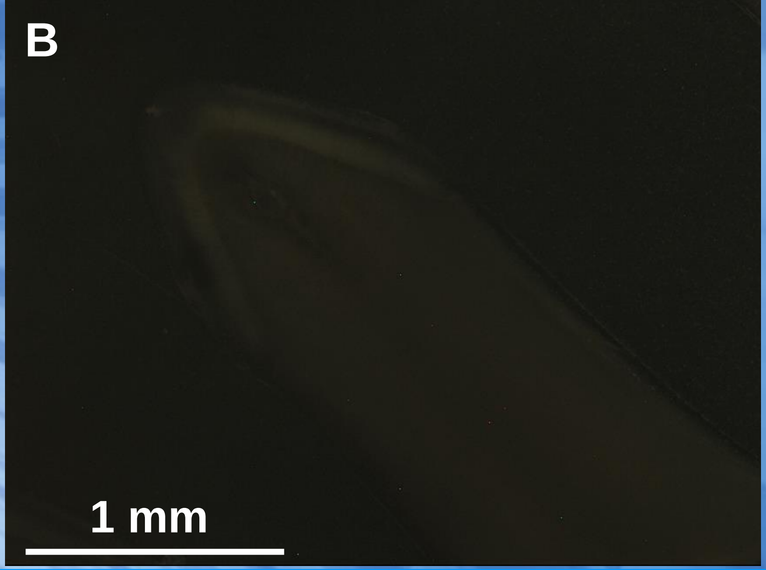

Transmitted light and hot cathodoluminescene images of a fish tooth (sample B; *Caturus* sp.; fossiliferous beds – D13, D14, unit III)

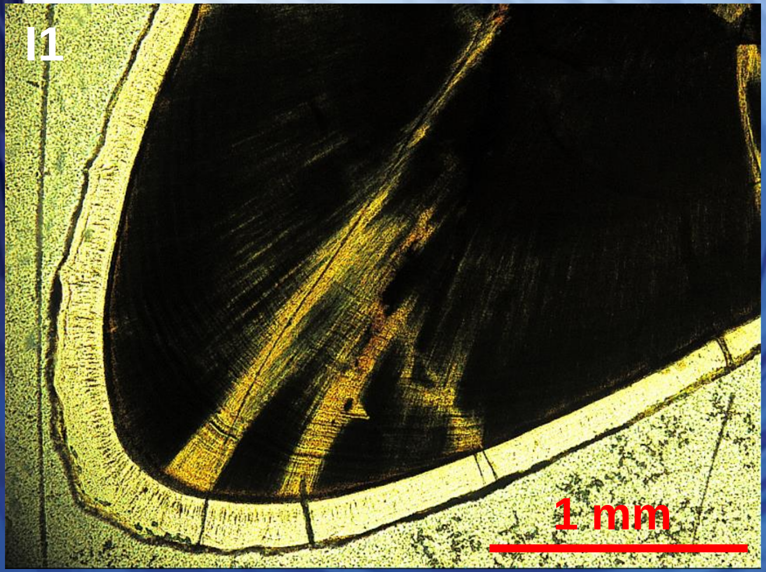

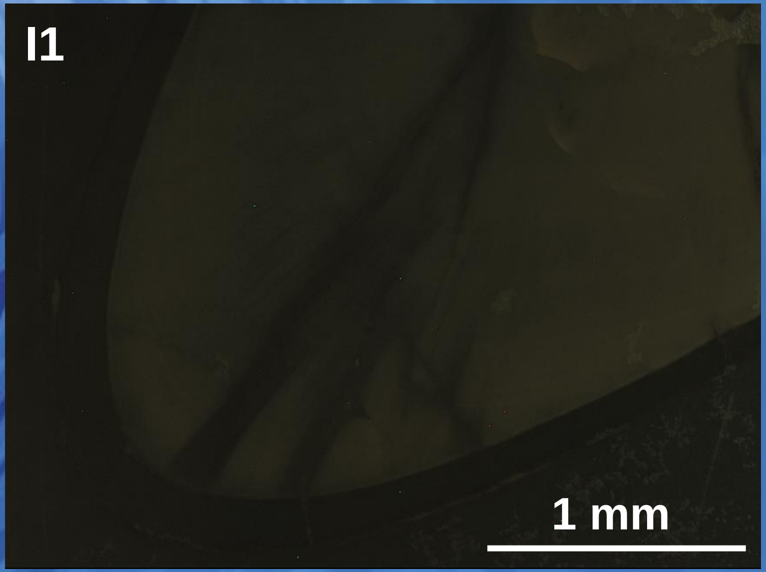

Transmitted light and hot cathodoluminescene images of an ichthyosaur tooth (sample I1; *C. kielanae;* a base of the Unit I)

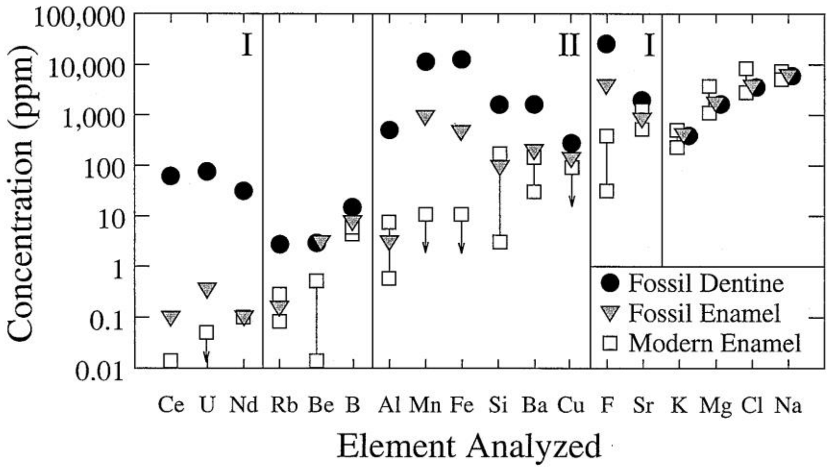

Concentrations of selected elements in well-preserved and altered mammal teeth (after Kohn et al. 1999)

Studied teeth show original fluoride contents in *Caturus* fish enameloid (3.7 wt.%) and a diagenetic incorporation of fluoride in *Caturus* fish dentine (3.1 wt.%) as well as ichthyosaur enamel (3.7 wt.%) and dentine (3.6 wt.%), which is an omnipresent process observed in hydroxyapatite skelatal remains of higher vertebrates (cf. de Renzi et al. 2016).

Fe and S concentartions in studied ichthyosaur and fish teeth measured using electron microprobe (CAMECA SX100). Enamel(oid) of both groups of teeth shows relatively low contents of Fe and S, which are incor-porated during diagenetic processes.

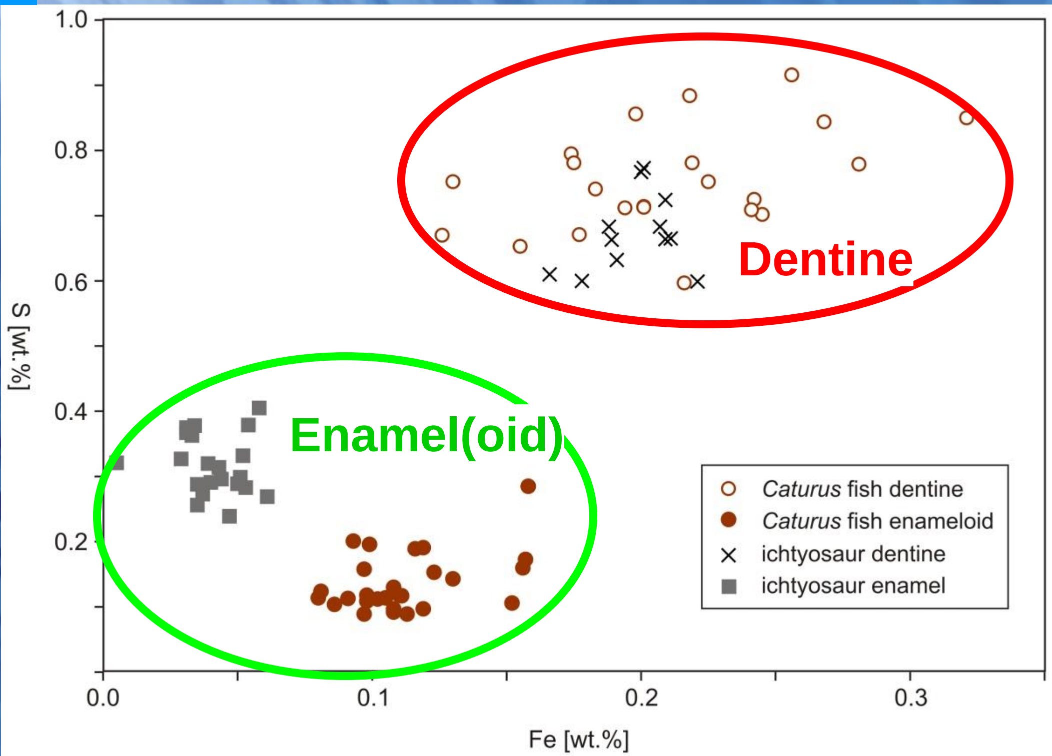

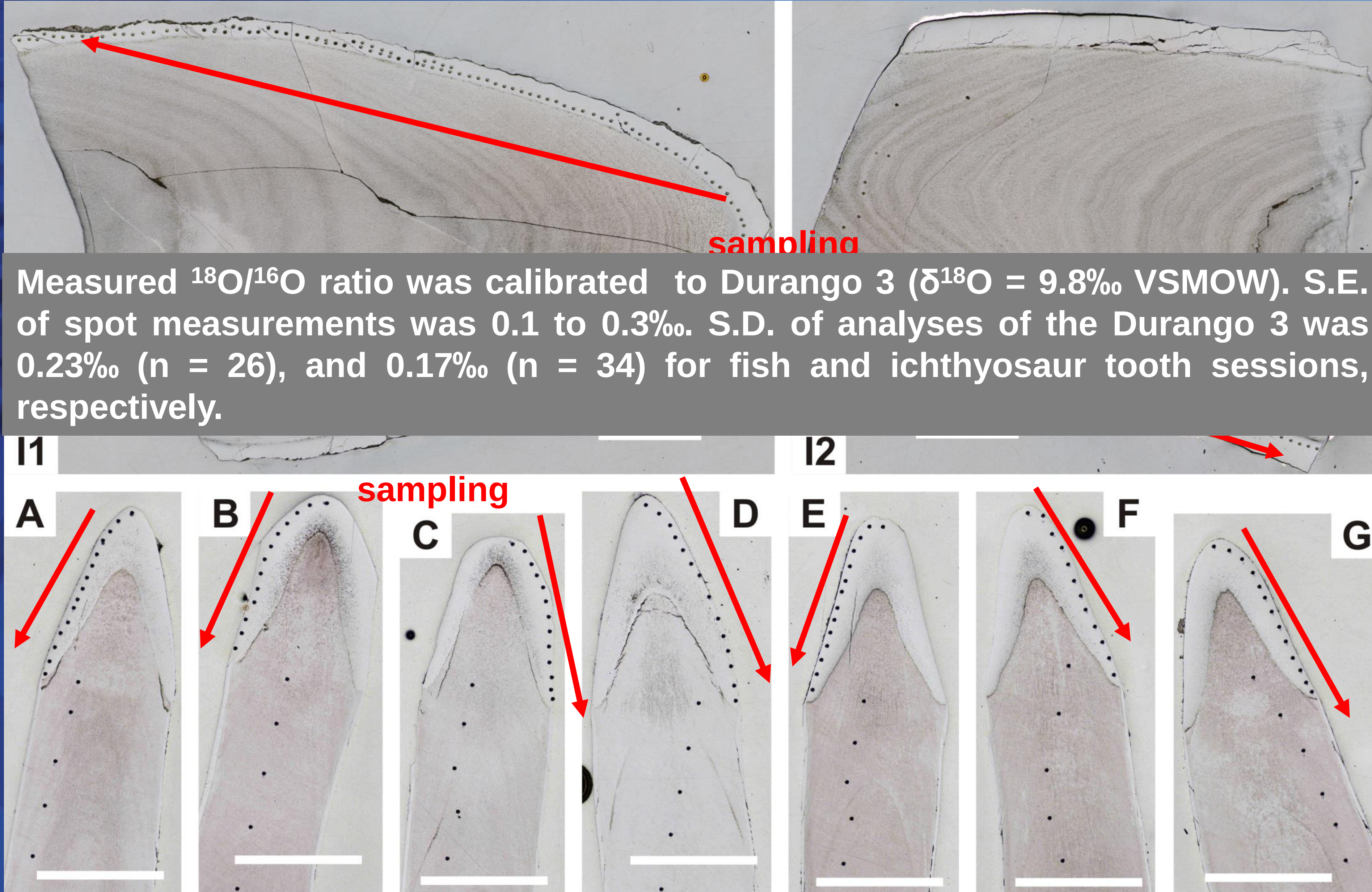

Measured $^{18}O/^{16}O$ ratio was calibrated to Durango 3 ($\delta^{18}O$ = 9.8‰ VSMOW). S.E. of spot measurements was 0.1 to 0.3‰. S.D. of analyses of the Durango 3 was 0.23‰ (n = 26), and 0.17‰ (n = 34) for fish and ichthyosaur tooth sessions, respectively.

Reflected light image of 2 ichthyosaur (*C. kielanae*; I1, I2) and 7 *Caturus* fish teeth (A, B, C, D, E, F, G) analysed for $\delta^{18}O$ values (at ca. 0.1 mm intervals) using a SHRIMP IIe/MC ion microprobe. Sampled spots are visible. Scale bars are 1 mm.

Respiratory enrichment of $\delta^{18}O$ value of body fluids (noted in water reptiles and mammals)

- **Small crocodilians – $\delta^{18}O$ value of body fluids similar to that of ambient water (Amiot et al. 2007)**
- **Larger crocodlians – $\delta^{18}O$ value of body fluids higher by 1.3 to 2‰ than that of ambient water (Amiot et al. 2007)**
- **Freshwater turtles – $\delta^{18}O$ value of body fluids higher by ca. 3.7‰ than that of ambient water (Amiot et al. 2007)**
- **Modern marine mammals show some viariability in $\delta^{18}O$ value of body fluids ($\Delta\ ^{18}O_{blood\text{-}water}$ amounts to ca. 0 ‰, 0.9 ‰ and 1.8‰ for pinnipeds, sea otters and cetaceans, respectively (Clementz and Koch, 2001)**

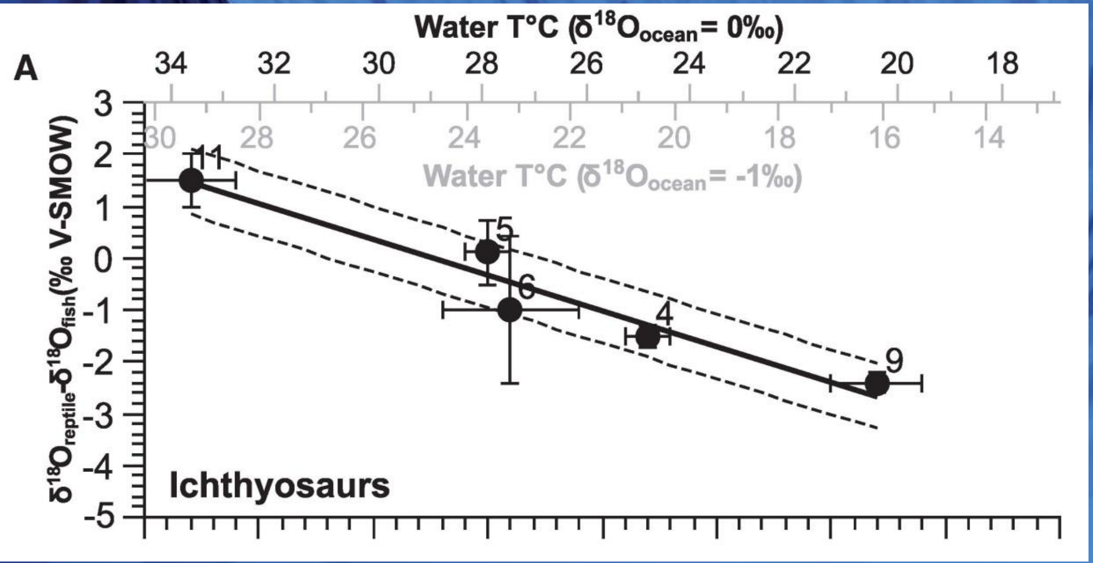

A comparison of $\delta^{18}O$ values of tooth enamel(oid) of coexisting fish and ichthyosaurs (assuming a small metabolic effect) suggest that these reptiles were endothermic and maintain the constant body temperatures of ca. 35°C (Bernard et al. 2010)

Ichthyosaurs were endothermic!

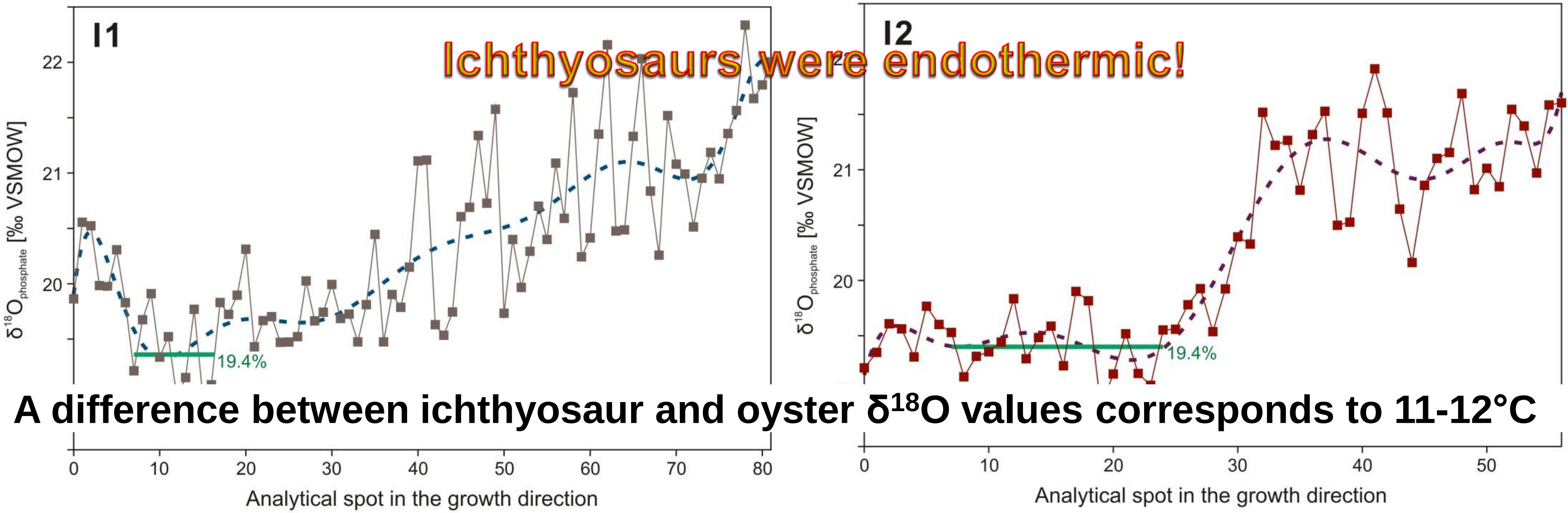

A difference between ichthyosaur and oyster $\delta^{18}O$ values corresponds to 11-12°C

$\delta^{18}O$ values of ontogenetic sections throughout the enamel of 2 ichthyosaur (*Cryopterygius kielanae*) teeth measured using SHRIMP IIe/MC. An increase of ca.

Assuming that a juvenile portion of ichthyosaur teeth is in isotope equilibrium with seawater and its body temperature of 35°C (after Bernard et al. 2010) it is possible to calculate $\delta^{18}O$ value of ambient water with an output of 1.1‰ VSMOW .

This value may be used to refine oyster isotope temperatures. Their $\delta^{18}O$ values (from -1 to 1‰ VPDB) translate into temperature range of 16 - 25°C (mean 21°C) using Anderson and Arthur (1983) equation.

These temperatures are consistent with palaeogeographic position of the Owadów-Brzezinki site (37°N; van Hinsbergen et al. 2015) and show slightly elevated salinity of the restricted mid-Polish basin during the latest Jurassic.

A new method of palaeotemperature calculation ?

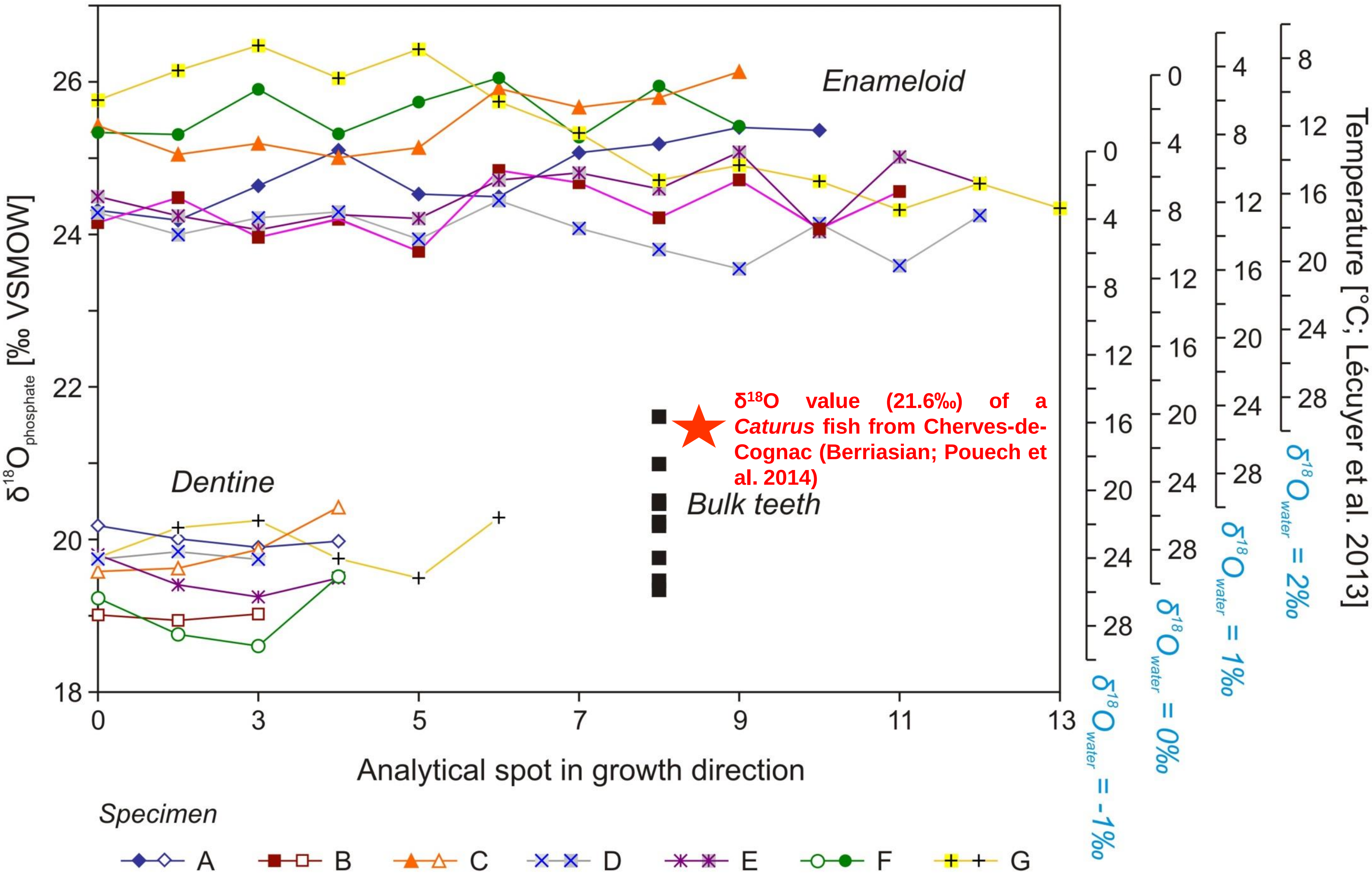

$\delta^{18}O$ values of ontogenetic sections throughout the enameloid and dentine of 6 *Caturus* fish teeth measured using SHRIMP IIe/MC and 10 bulk *Caturus* teeth measured using the standard TC EA method

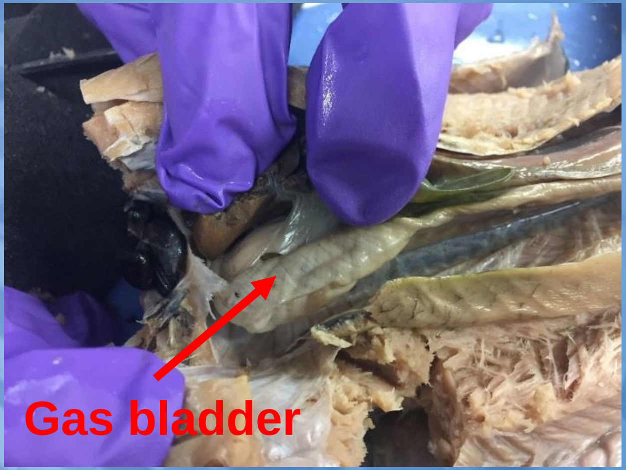

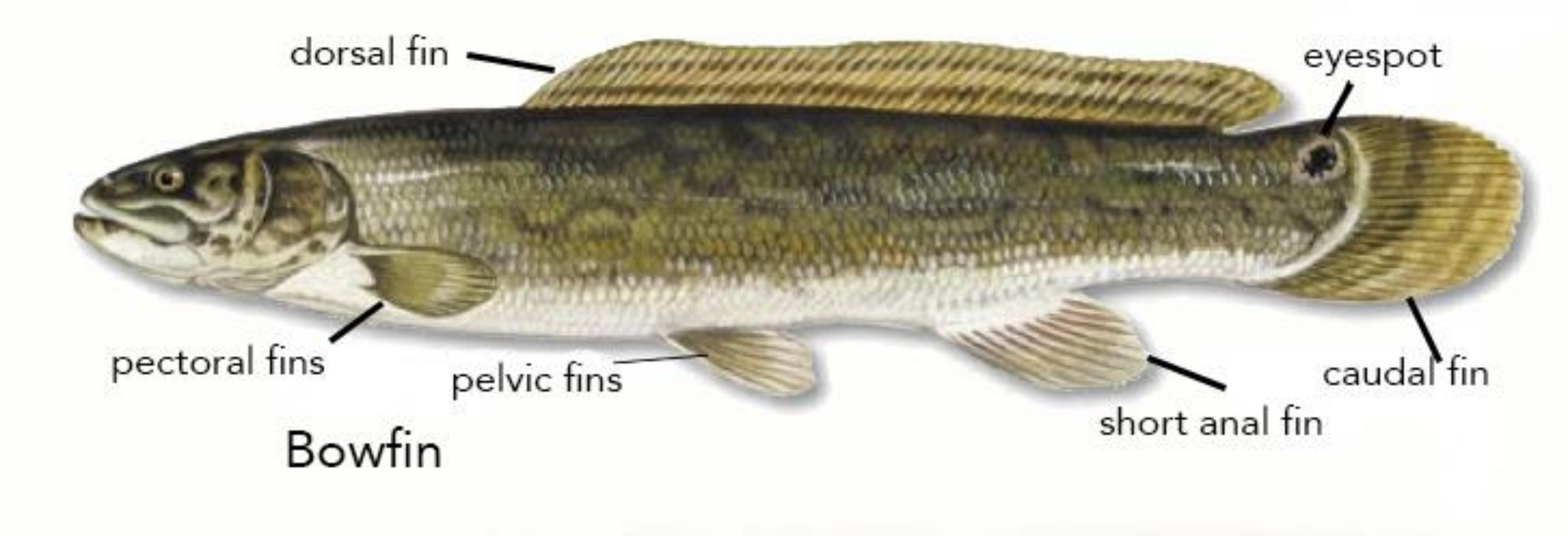

Modern counterparts of Caturus fishes i.e. bowfins (*Amia calva)* are bimodal breathers. Their gills exchange gases in the water, they also have a gas bladder that can serve to breathe air using a small pneumatic duct connected to its foregut. They can break the surface to gulp air, which allows them to survive conditions of aquatic hypoxia that are lethal to other species (after Wikipedia; https://en.wikipedia.org/wiki/Bowfin).

- Depositional environments of the Owadów-Brzezinki basin varied from offshore and nearshore (Brzostówka marls, unit I limestones) to coastal and lagoonal ones (units II, III, IV). The latter palaeoenvironments were characterised by high-amplitude variations in seawater salinities and oxygenation level of bottom waters, which favoured the preservation of fragile fossils.
- Results of microsampling of oyster shells (using a MicroMill device) show that the intrashell range of (-1 to 1‰ VPDB) is slightly higher than the range of bulk oyster $\delta^{18}O$ values. The $\delta^{18}O$ variations may be linked to seasonal changes in both temperature and salinity of the sedimentary basin.
- Results of microsampling of ichthyosaur teeth by a SHRIMP IIe/MC ion microprobe have confirmed endothermy of these reptiles. A juvenile portion of the enamel is probably precipitated close to the oxygen isotope equilibrium and may be used for the determination of ambient water $\delta^{18}O$ value, which is crucial for palaeoclimatic studies.
- Results of microsampling of *Caturus* tooth enameloid by a SHRIMP IIe/MC ion microprobe show high $\delta^{18}O$ values (ca. 25‰VSMOW) that may be linked to either elevated salinities of water [illegible] in oxygen-depleted environment. This imposes re-interpretation of the habit of these fishes.

Thank you for your attention!

REFERENCES

- AMIOT, R., LÉCUYER, C., ESCARGUEL, G., BILLON-BRUYAT, J.-P., BUFFETAUT, E., LANGLOIS, C., MARTIN, S., MARTINEAU, F., AND MAZIN, J.-M., 2007, Oxygen isotope fractionation between crocodilian phosphate and water: Palaeogeography, Palaeoclimatology, Palaeoecology, v. 243, p. 412–420.
- ANDERSON, T.F., AND ARTHUR, M.A., 1983, Stable isotopes of oxygen and carbon and their application to sedimentologic and paleoenvironmental problems, in Arthur, M.A., Anderson, T.F., Kaplan, I.R., Veizer, J., and Land, L.S. (eds.), Stable Isotopes in Sedimentary Geology: SEPM Short Course No. 10, Dallas, p. 1-1–1-151.
- BERNARD, A., LÉCUYER, C., VINCENT, P., AMIOT, R., BARDET, N., BUFFETAUT, E., CUNY, G., FOUREL, F., MARTINEAU, F., MAZIN, J.-M., AND PRIEUR, A., 2010, Regulation of body temperature by some Mesozoic marine reptiles: Science v. 328, p. 1379–1382.
- CLEMENTZ, M.T., AND KOCH, P.L., 2001, Differentiating aquatic mammal habitat and foraging ecology with stable isotopes in tooth enamel: Oecologia, v. 129, p. 461–472.
- DE RENZI, M., MANZANARES, E., MARIN-MONFORT, M.D., AND BOTELLA, H., 2016, Comments on “Dental lessons from past to present: ultrastructure and composition of teeth from plesiosaurs, dinosaurs, extinct and recent sharks” by A. Lübke, J. Enax, K. Loza, O. Prymak, P. Gaengler, H.-O., Fabritius, D. Raabe and M. Epple, *RSC Adv.*, 2015, 5, 61612: RSC Advances, v. 6, p. 74384–74388.

- Kim, S.-T., and O'Neil, J.R., 1997, Equilibrium and nonequilibrium oxygen isotope effects in synthetic carbonates: Geochemica et Cosmochimica Acta, v. 61, p. 3461–3475.
- Kin, A., Gruszczyński, M., Martill, D., Marshall, J.D., and Błażejowski, B., 2013, Palaeoenvironment and taphonomy of a Late Jurassic (Late Tithonian) Lagerstätte from central Poland: Lethaia, v. 46, p. 71–81.
- Lécuyer, C., Amiot, R., Touzeau, A., and Trotter, J., 2013. Calibration of the phosphate $\delta^{18}O$ thermometer with carbonate-water oxygen isotope fractionation equations: Chemical Geology, v. 347, . 217–226
- Nunn, E.V., and Price, G.D., 2010, Late Jurassic (Kimmeridgian–Tithonian) stable isotopes ($\delta^{18}O$, $\delta^{13}C$) and Mg/Ca ratios: new paleoclimate data from Helmsdale, Northeast Scotland: Palaeogeography, Palaeoclimatology, Palaeoecology, v. 292, p. 325–335.
- Railback, L.B., Anderson, T.F., Ackerly, S.C. & Cisne, J.L. 1989, Paleoceanographic modeling of temperature-salinity profiles from stable isotopic data. – Paleoceanography, v. 4, p. 585–591.
- Rohling, E.J., 2013, Oxygen Isotope Composition of Seawater. Encyclopedia of Quaternary Science, v. 2, p. 915–922.
- van Hinsbergen D.J.J., de Groot L.V., van Schaik S.J., Spakman W., Bijl P.K., Sluijs A., Langereis, C.G., and Brinkhuis, H., 2015, A paleolatitude calculator for paleoclimate studies: Plos One, v. 10, e0126946.

- **Wierzbowski, H., Anczkiewicz, R., Pawlak, J., Rogov, M.A., and Kuznetsov, A.B., 2017, Revised Middle–Upper Jurassic strontium isotope stratigraphy: Chemical Geology, v. 466, p. 239–255.**
- **Wierzbowski, H., Dubicka, Z., Rychliński, T., Durska, E., Olempska, E., and Błażejowski, B., 2016, Depositional environment of the Owadów-Brzezinki conservation lagerstätte (uppermost Jurassic, central Poland): evidence from microfacies analysis, microfossils and geochemical proxies: Neues Jahrbuch für Geologie und Paläontologie – Abhandlungen, v. 282, p. 81–108.**
- **Zhou, J., Poulsen, C.J., Pollard, D., White, T.S., 2008, Simulation of modern and middle Cretaceous marine $\delta^{18}O$ with an ocean-atmosphere general circulation model. Paleoceanography, v. 23, PA3223.**